ADDIS ABABA UNIVERSITY
SCHOOL OF GRADUATE STUDIES
DEPARTMENT OF MECHANICAL ENGINEERING

EXPERIMENTAL ANALYSIS FOR PERFORMANCE EVALUATION OF SOLAR DRYER

By

Aklilu Tesfamichael

Approved by Board Examiners:

Dr-Ing. Demiss Alemu _____
Chairman, Department Graduate Committee

Dr-.Ing. Abebayehu Assefa _____
Advisor

Dr. Rajendra Karwa _____
External Examiner

Dr-Ing. Demiss Alemu _____
Internal Examiner

Acknowledgments

The completion of this thesis would not have been possible without the help of several people. First, I would like to thank my God for guiding me throughout the journey of my life. My gratitude, love, and respect go out to all my caring and understanding family.

I also thank Dr.-Ing Abebayhu Assefa, my advisor for this project and who has taught me many courses. His advice and guidance for my research and contribution to my education has been invaluable. I thank Dr.-Ing Demiss Alemu, for the inspiration and encouragement to work on this project. My thanks also go out to Dr. Rajandar Karwa, for his, advice and availing articles.

I also thank the entire working group in mechanical workshop (especially Ato Kassaye Negash) and Ato Daniel Kefli who supplied me with weighing device.

Last but not least, the equipment facilities presented by the Solar Energy Research and Development Group of Faculty of Technology, AAU, is acknowledged.

Table of Contents

List of Table

List of Figures

Abstract

An experimental set up has been developed to investigate the performance of natural convection solar dryer for drying of selected material. Measurements of total solar radiation on the plane of the collector, ambient temperature and humidity, air flow rate, temperature and relative humidity inside the dryer as well as solid's moisture loss-in-weight data are employed to study the performance of the dryer. A data logger and a computer were employed for data acquisition. First, detailed diagnostic experiments were carried out with no drying material on the trays. Next, a number of experiments were conducted using potato slices. For all the test conditions, the material gets dried with system's efficiency of 15.9%. The drying time compared to sun drying was reducing by about 19%. The protection of the dried material against direct sunshine, dust, and insects results better quality product.

Chapter 1

Introduction

1.1 Overview and Objective of the Thesis

Food scientists have found that by reducing the moisture content of food to between 10 and 20%, bacteria, yeast, mold and enzymes are prevented from spoiling it. The flavor and most of the nutritional value is preserved and concentrated [16].

Wherever possible, it is traditional to harvest most grain crops during a dry period or season and simple drying methods such as sun drying are adequate. However, maturity of the crop does not always coincide with a suitably dry period. Furthermore, the introduction of high-yielding varieties, irrigation, and improved farming practices have led to the need for alternative drying practices to cope with the increased production, and grain harvested during the wet season as a result of multi-cropping.

Drying and preservation of agricultural products have been one of the oldest uses of solar energy. The traditional method, still widely used throughout the world, is open sun drying where diverse crops, such as fruits, vegetables, cereals, grains, tobacco, etc. are spread on the ground and turned regularly until sufficiently dried so that they can be stored safely.

However, there exist many problems associated with open sun drying. It has been seen that open sun drying has the following disadvantages. It requires both large amount of space and long drying time. The crop is damaged because of the hostile weather conditions, contamination of crops from the foreign materials, degradation by overheating, the crop is subject to insect infestation, the crop is susceptible to re-absorption of moisture if it is left

on the ground during periods of no sun, and there is no control on the drying process. This could lead to slow drying rate, contamination and poor quality of dried products, and loss in production. Although the spreading of the crop on the ground or on a platform and drying it directly by the sun is cheap and successfully employed for many products throughout the world, where solar radiation and climatic conditions are favorable, because of the above mentioned factors of open sun drying process and a better understanding of the method of utilizing solar energy to advantage, have given rise to a scientific method called solar drying.

Solar drying of farm crops offers the following advantages by permitting: early harvest which reduces the field loss of products from storm and natural shattering. The field conditions (dry and fewer weeds) are often better for harvesting earlier in the season, planning the harvesting season to make better use of labor. Farm crops can be harvested when natural drying conditions are unfavorable. Long-time storage with little deterioration. Extended storage periods are becoming increasingly important with large amount of grain being stored and carried over through another storage year by the farmer, government, and industry, and the farmer's taking advantage of higher price a few months after harvest although in some years there may be no price advantage. By removing moisture the possibility of the grain heating with subsequent reduction or destruction of germination is decreased. The farmer's selling a better quality product which is worth more to him and to those who must use those products [2].

Therefore, by providing a sheltered drying area or chamber in which the crops to be dried and stored, a stream of air is heated by solar energy to reduce its relative humidity which is

then passed over the crops. This form of solar drying could improve the quality of the crop to be dried, reduce spoilage by contamination and local overheating, reduce spillage losses, speed up the drying process, achieve better quality control, and reduction in drying time.

The disadvantages of open sun drying need an appropriate technology that can help in improving the quality of the dried products and in reducing the wastage. This led to the application of various types of drying devices like solar dryer, electric dryers, woodfuel driers and oil-burned driers. However, the high cost of oil and electricity and their scarcity in the rural areas of most third world countries have made some of these driers very unattractive. Therefore interest has been focused mainly on the development of solar driers [23].

Solar dryers are usually classified according to the mode of air flow into natural convection and forced convection dryers. Natural convection dryers do not require a fan to pump the air through the dryer. The low air flow rate and the long drying time, however, result in low drying capacity. Thus, this system is restricted to the processing of small quantities of agricultural surplus for family consumption. Where large quantities of fresh produce are to be processed for the commercial market, forced convection dryers should be used [1].

One basic disadvantage of forced convection dryers lies in their requirement of electrical power to run the fan. Since the rural or remote areas of many developing countries are not connected to the national electric grids, the use of these dryers is limited to electrified urban areas. Even in the urban areas with grid-connected electricity, the service is unreliable. In view of the prevailing economic difficulties in most of these countries, this situation is not

expected to change in the foreseenable future. The use of natural convection solar dryer could boost the dissemination of solar dryers in the developing countries [1]. Therefore, experimental performance of solar dryer has been evaluated in this thesis.

1.2 Literature Review

Drying of agricultural dates back to the beginning of civilization. The use of the solar energy and air movement provided the major method of moisture removal in the field. Crops for human consumption were occasionally dried in ovens or by hanging in heated rooms. Between World War I and II, several experimental mechanical drying units were built and a few commercial units were in operation. Commercial dryers were primarily used for dehydration of fruits, vegetables, and hay, drying of seed corn with heated air, and drying hay in the barn, usually with unheated forced air. Commercial and large scale farm drying became a common practice after World War II. The increase in drying was coupled to the rapid increase in mechanization and increase in land labor productivity. Large quantities of moist or wet products were produced at harvest requiring moisture removal to avoid loss during subsequent handling and storing. Speed of operations from harvest to storage forced the consideration, study, and use of heated air for drying [2].

Literature survey was outlined by S. Soponronnarit [21] as follows, "*Wibulswas et al. [1977] found that the drying rate of wet cloth in a convection solar cabinet dryer was about 4.2 kg/m^2-day. Watabutr [1981] found that the maximum drying efficiency occurred when the ratio of outlet area to solar receiving area was 11 per cent (the inlet area was much greater than the outlet area) and the slope of the glass cover was 14º, yielding a*

drying rate of about 3.2 kg/m^2–day using box dryer. Drying of banana in a solar cabinet took three days and better quality product was obtained as compared with that in the case of direct sun drying [Anon, 1979].

Wibulswas and Thaina [1980] tested a mixed mode natural convection solar dryer and found that the drying rate of wet cloth was 5 kg/m^2–day. The maximum drying efficiency occurred when the ratio of outlet area to absorbing area was 0.8 per cent. Patranon [1984] conducted in-field solar drying using dryers similar to that of Wibulswas and Thaina [1980]. The products dried were banana, fish, meat and coconut. Exell [1980] developed a low-cost mixed mode natural convection solar dryer for paddy-drying. Paddy could be dried safely in 2-3 days.

Solar air heaters which were integrated in natural convection solar dryers have also been investigated. These were plastic film solar air heaters used in a solar rice dryer [Exell, 1980], and a flat-plate solar air heater in a cabinet solar dryer [Wibulswas and Haina, 1980; Patranon, 1984]. Due to natural convection of air through the solar air heater, the air flow rate varies. Hence, thermal efficiency varies throughout the day. The solar collection efficiency is usually less than in the case of forced convection.''

Some recommended drying temperatures are: fruits and vegetables: 38- 55^{0}C; temperature over 65^{0}C can result in sugar caramelization of many fruit products; fish 60-66^{0}C; rice, grains, seeds, brewery grains: 45^{0}C maximum temperature [16].

1.3 Objectives of the Research

The general objective of this thesis is experimental investigation of the components of free convection solar drying systems which involve consideration of solar collector and drier. In this thesis, the analysis will concentrate on the practical field test performance of the existing, locally manufactured, solar dryer using the state of the art equipment recently available for solar energy research and development program of the Faculty of Technology. The experiment is conducted in the Addis Ababa University, Faculty of Technology.

In this paper, the variables and mechanisms involved in the dehydration processes would be discussed. The drying time of the dryer is also compared with the open sun drying time.

1.4 Thesis Direction

Earlier works on solar drying are outlined in the literature review. The research to be described in the rest of this thesis proceeds as follows: The second chapter focuses on the literature survey of different drying theories, like drying mechanism, drying air properties, types of solar dryers and drying efficiency. The third chapter deals with test set-up and installation of the measuring devices such as thermocouples, relative humidity sensors, and pyranometer with the data logger. The fourth chapter describes the procedure of the experiment. The fifth and sixth chapters deal with the analysis of results, and conclusion and recommendations, respectively.

Chapter 2

Theory of Solar Dryer

Solar drying refers to a technique that utilizes incident solar radiation to convert it into thermal energy required for drying purposes. Most solar dryers use solar air heaters and the heated air is then passed through the drying chamber (containing material) to be dried. The air transfers its energy to the material causing evaporation of moisture of the material.

2.1 Drying Mechanism

In the process of drying, heat is necessary to evaporate moisture from the material and a flow of air helps in carrying away the evaporated moisture. There are two basic mechanisms involved in the drying process: the migration of moisture from the interior of an individual material to the surface, and the evaporation of moisture from the surface to the surrounding air. The drying of a product is a complex heat and mass transfer process which depends on external variables such as temperature, humidity and velocity of the air stream and internal variables which depend on parameters like surface characteristics (rough or smooth surface), chemical composition (sugars, starches, etc.), physical structure (porosity, density, etc.), and size and shape of products. The rate of moisture movement from the product inside to the air outside differs from one product to another and depends very much on whether the material is hygroscopic or non-hygroscopic. Non-hygroscopic materials can be dried to zero moisture level while the hygroscopic materials like most of the food products will always have a residual moisture content. This moisture, in hygroscopic material, may be a bound moisture which remained in the material due to

closed capillaries or due to surface forces and unbound moisture which remained in the material due to the surface tension of water as shown in Figure 2.1 [14].

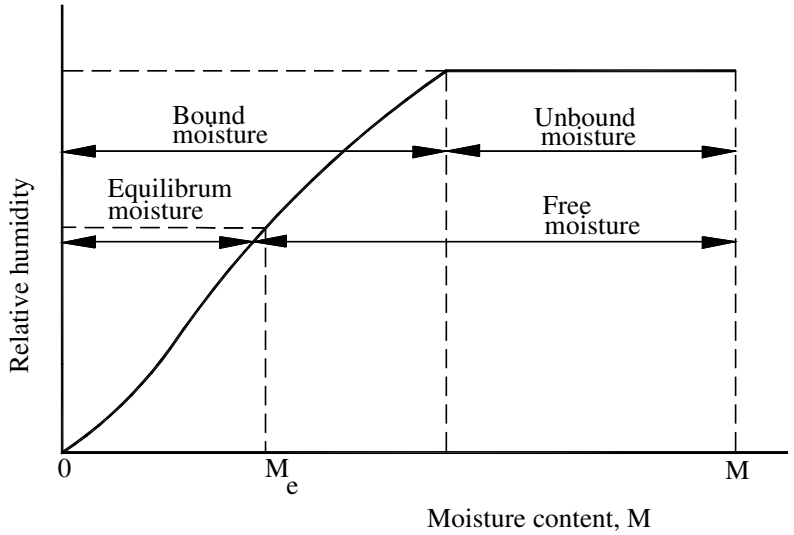

Figure 2.1 Moisture in the drying material.

When the hygroscopic material is exposed to air, it will absorb either moisture or desorb moisture depending on the relative humidity of the air. The equilibrium moisture content (EMC = M_e) will soon reach when the vapour pressure of water in the material becomes equal to the partial pressure of water in the surrounding air [14]. The equilibrium moisture content in drying is therefore important since this is the minimum moisture to which the material can be dried under a given set of drying conditions. A series of drying characteristic curves can be plotted. The best is if the average moisture content M of the material is plotted versus time as shown in Figure 2. 2.

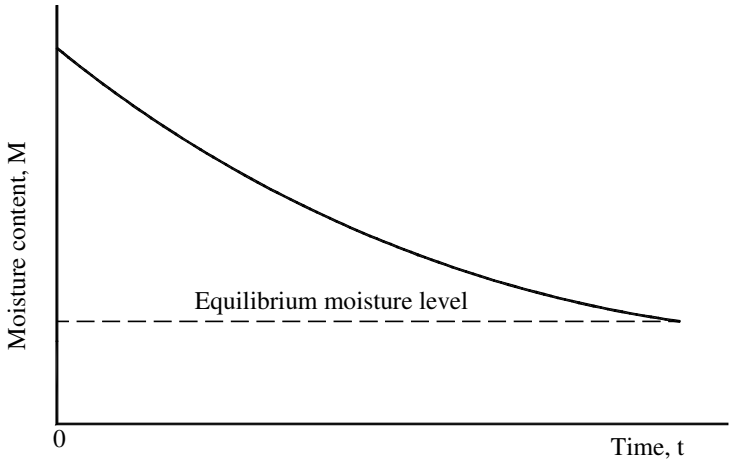

Figure 2.2 Rate of moisture loss

Another curve can be plotted between drying rate i.e. dM/dt versus time t as shown in Figure 2.3. But more information can be obtained if a curve is plotted between drying rate dM/dt versus moisture content M as shown in Figure 2.4.

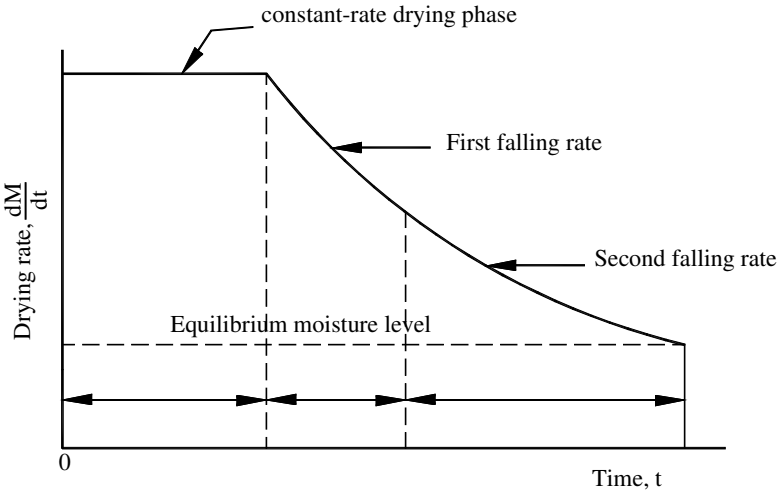

Figure 2.3 Drying rate with time curve

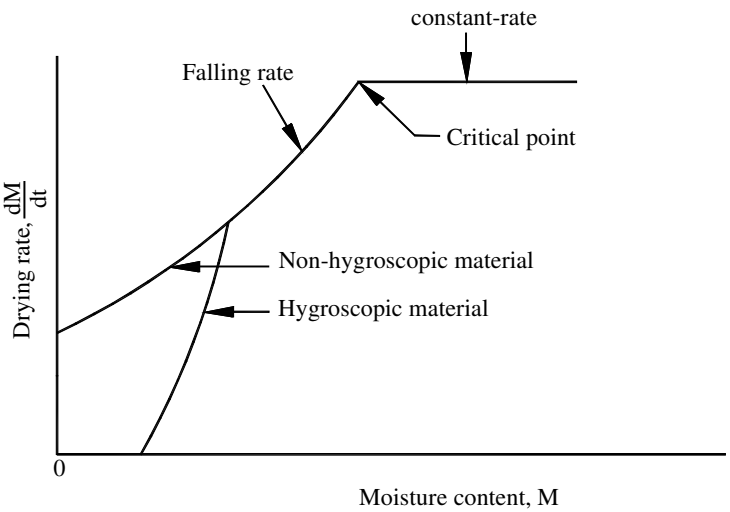

Figure 2.4 Typical drying rate curve

As is seen from Figure 2.4 for both non-hygroscopic and hygroscopic materials, there is a constant drying rate terminating at the critical moisture content followed by falling drying rate. The constant drying rate for both non-hygroscopic and hygroscopic materials is the same while the period of falling rate is little different. For non-hygroscopic materials, in the period of falling rate, the drying rate goes on decreasing till the moisture content become zero. While in the hygroscopic materials, the period of falling rate is similar until the unbound moisture content is completely removed, then the drying rate further decreases and some bound moisture is removed and continues till the vapour pressure of the material becomes equal to the vapour pressure of the drying air. When this equilibrium reaches then the drying rate becomes zero [14].

The period of constant drying for most of the organic materials like fruits, vegetables, timber, etc. is short and it is the falling rate period in which is of more interest and which depends on the rate at which the moisture is removed. In the falling rate regime moisture is migrated by diffusion and in the products with high moisture content, the diffusion of moisture is comparatively slower due to turgid cells and filled interstices. In most agricultural products, there is sugar and minerals of water in the liquid phase which also

migrates to the surfaces, increase the viscosity hence reduce the surface vapour pressure and hence reduce the moisture evaporation rate [14].

Drying is done either in thin layer drying or deep layer drying. In thin layer drying; which is done in case of most of fruits and vegetables, the product is spread in thin layers with entire surface exposed to the air moving through the product and the Newton's law of cooling is applicable in the falling rate region. Most of the grains are dried in deep layer which can be considered as a series of thin layers and the temperature and the humidity varies from layer to layer [14].

2.2 Air Properties

The properties of the air flowing around the product are major factors in determining the rate of removal of moisture. The capacity of air to remove moisture is principally dependent upon its initial temperature and humidity; the greater the temperature and lower the humidity the greater the moisture removal capacity of the air. The relationship between temperature, humidity and other thermodynamic properties is represented by the psychrometric chart. It is important to appreciate the difference between the absolute humidity and relative humidity of air. The absolute humidity is the moisture content of the air (mass of water per unit mass of air) whereas the relative humidity is the ratio, expressed as a percentage, of the moisture content of the air at a specified temperature to the moisture content of air if it were saturated at that temperature.

The changes in condition of air when it is heated using the solar energy and then passed through a bed of moist product are shown in Figure 2.5. The heating of air from temperature T_A to T_B is represented by the line AB. During heating the absolute humidity remains constant at ω_A whereas the relative humidity falls from ϕ_A to ϕ_B. As air moves

through the material to be dried, it absorbs moisture. Under (hypothetical) adiabatic drying; sensible heat in the air is converted to latent heat and the change in the condition of air is represented along a line of constant enthalpy, BC. Both absolute humidity and relative humidity increase from ω_B and ω_C and from ϕ_B to ϕ_C, respectively, but air temperature decreases to, T_C. The absorption of moisture by the air would be the difference between the absolute humidities at C and B. ($\omega_C - \omega_A$). If unheated air is passed through the bed, the drying process would be represented by the line AD. Assuming that the air at D to be at the same relative humidity, ϕ_C, as the heated air at C, then the absorbed moisture would be ($\omega_D - \omega_A$), considerably less than that absorbed by the heated air ($\omega_C - \omega_A$).

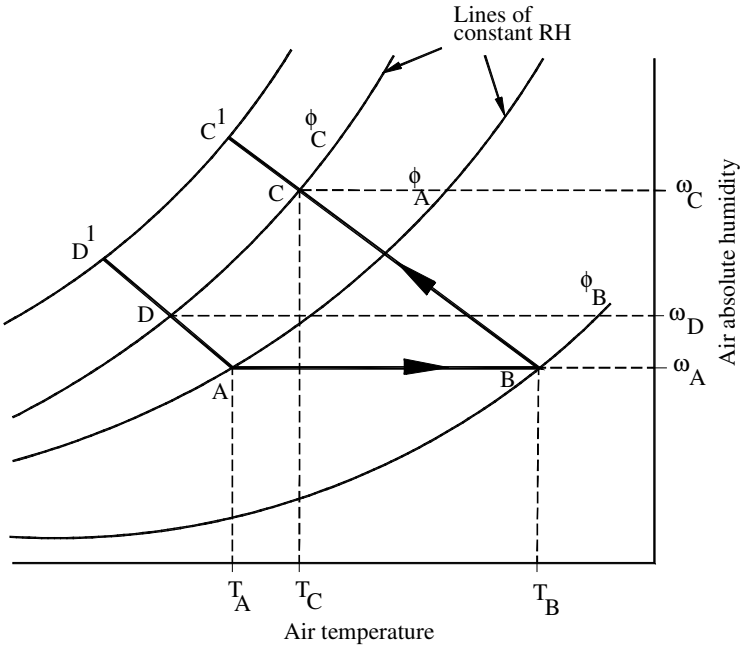

Figure 2.5 Representation of drying process

2.3 Types of Solar Dryers

There are a large variety of solar dryers. These solar dryers have been classified in many ways. Considering the operational modes and practicability of dryers, they can be classified basically into two types: natural convection type dryers and forced circulation type dryers [14].

2.3.1 Natural Convection Solar Dryers

These dryers appear to be more attractive for use in developing countries since they do not use any fan or blower to be operated by electrical energy. Moreover, they are low in cost and easy to operate. However, the problems with these dryers are: slow drying, not much control on temperature and humidity, small quantities can be dried, and some products, due to direct exposure to sun, change colour and flavour. In its simple form, it consists of some kind of enclosure and a transparent cover. The food product gets heated due to direct absorption of heat or due to high temperature in the enclosure and therefore moisture from the product evaporates and goes out by natural circulation of air.

2.3.1.1 Rack Type Solar Dryer

The dryer consists of racks of certain width, length, and some spacing made of wire mesh over which the drying material is placed and covered at the top by a metal or wooden roof to protect the material from rain and excessive sun.

2.3.1.2 Solar Cabinet Dryer or Box Dryer

The simplest solar dryers are the cabinet dryers (Figure 2.6). Their main characteristic is that the heat needed for drying gets into the material through direct radiation and through a

south-oriented, transparent (glass or foil) wall 1. Other walls of the dryer are opaque and well insulated.

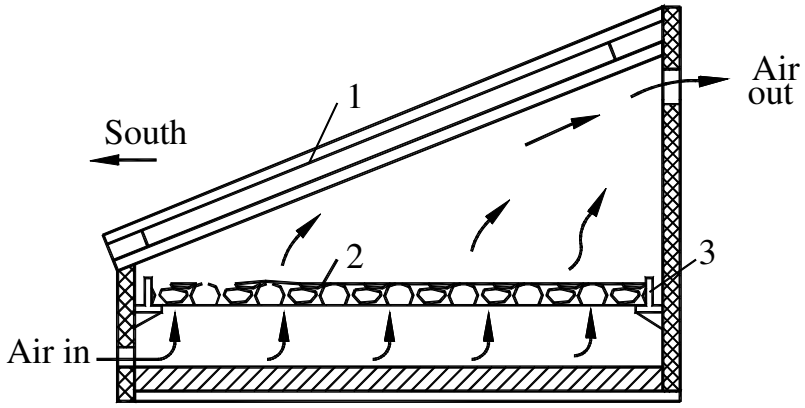

Figure 2.6 Structure of a cabinet dryer

The drying material 2 is spread in a thin layer on a tray 3. The bottom plate of the tray is perforated. Air flows through the holes by natural convection through the material and finally leaves through the upper part of the cabinet (Figure 2.6). The design of the dryer is simple, and its cost is low. It is suitable for drying small quantities (10-20 kg) of granular materials (e.g., for individual farmers). The products dried in cabinet dryers are mainly agricultural products, vegetables, fruits, spices, and herbs. Drying of the material can be made more even by periodic turning over of the material. It is employed chiefly in tropical countries, but during the warm months it can be used in the temperate climates as well. The usual size of the drying area is 1-2 m^2 [13].

2.3.1.3 Green House Type Solar Dryer

This dryer appears to look like a small greenhouse (Figure 2.7) where there are two parallel long drying platforms made of wire mesh and are covered with slanted long glass roof with

long axis along the north-south direction. There is a metallic cap at the top of the glass roof leaving some space in between through which moist warm air can go out creating partial vacuum inside and therefore fresh outside air is sucked through holes provided on the side walls facing east and west below the drying platforms. This cap doesn't allow rain and dust to enter the dryer and enhances the moisture evaporation from the product. The inside of the dryer as well the trays are painted black. Fresh air in the dryer enters through the openings through shutters provided in the lower portion of the walls below the glass roof and above the drying platforms. Solar radiation penetrates through the glass roof, heats the product directly and absorbed within the dryer increasing the inside temperature [14].

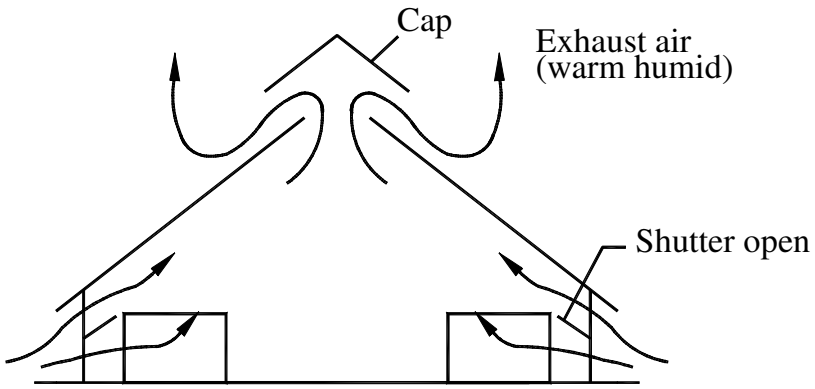

Figure 2.7 Green house type solar dryer

2.3.2 Indirect Type Solar Dryers

The capacity per unit area of cabinet dryer is limited by two conditions: need for direct radiation on the drying materials and small airflow rate. To dry large quantities of material, the basic area of the dryer has to be increased. To avoid this problem it is preferable to

place the material in several independent layers; the necessary heat transfer is thus accomplished by convection. The increase in mass flow rate of the air can be achieved by increasing the effects that produce natural convection. These effects must also be increased if the air is to be circulated through a material laid in several layers one over the other, or through a thick layer, as in the case of the chimney type. To keep up without using a ventilator (for instance, in a field), the "chimney effect must be exploited". For this purpose the vertical flow of hot air in the dryer must be increased.

2.3.2.1 Shelf Type Dryer

In Figure 2.8, a schematic view of the so-called shelf dryer is shown. As can be seen in Figure 2.8, the material to be dried is placed on perforated shelves ,1, built one above the other. The front wall of the case faces south, its top and sides ,2, are covered by transparent walls (glass or sheet), and the back wall ,3, is heat insulated. The back wall and the floor are covered with a coating of black paint. The ambient air is warmed in a flat-plate collector ,4, joined to the bottom of the case, and it flows up to the space under the lowest shelf. Moist air exits to the open through the upper opening of the casing ,5,. In the scheme shown in Figure 2.8, the chimney effect is ensured by the increased height of the dryer.

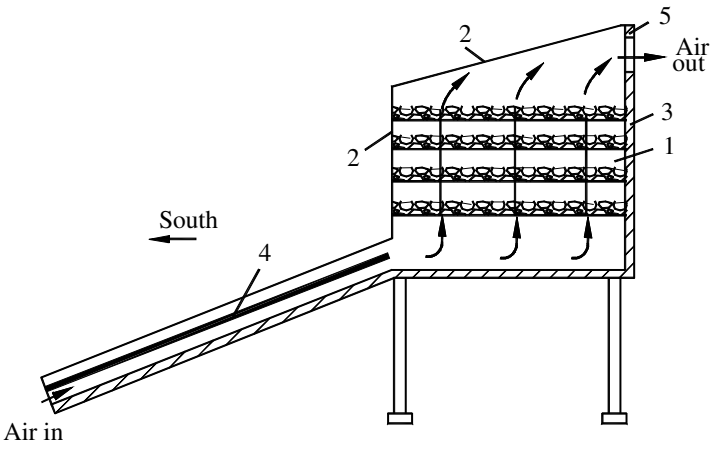

Figure 2.8 Shelf-type dryer with separate collector

The experiments indicated that separation of the collector is only justified with a high efficiency collector. This dryer is suitable for drying fruits and vegetables [13].

2.3.2.2 Chimney Type Paddy Dryer

For large amounts of material, an appropriately high chimney has to be connected to the dryer housing. Figure 2.9 gives cross-section of chimney type dryer designed and built for drying 1000 kg rice. Rice is placed in a static bed ,1, in a 0.1 m thick layer. The collector consists of a plastic covering and roasted rice shell, the latter playing the role of absorber. The front surface ,3, over the layer of the rice is also transparent. The wall of the chimney, 5, is made of black plastic foil. The frame work of the dryer is wood and wire. Manufacture of the unit is inexpensive and simple. The air needed for drying amounts to 5.7 m^3/min per m^3 rice. The chimney is ,5, m high. Drying is not uniform, so the rice in the static bed must be turned over at intervals. The duration of the drying is 3-4 days in the case of 15MJ/m^2, day mean global sun radiation, and 23 m^2 collector surface. With the application of a large (36 m^2) collector surface, drying time can be reduced to 1-2 days in good weather. As a rule of thumb, the solar collector surface must be approximately three times the surface of the bed [13].

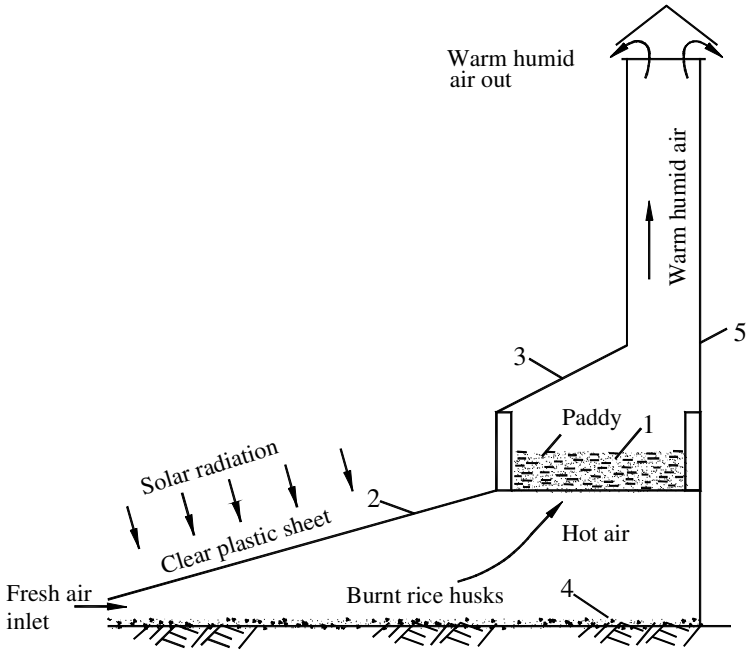

Figure 2.9 Cross section of chimney type paddy dryer

2.4 Key Elements of Solar Dryer

The indirect free convection solar dryer used in this research work has the following major components. The solar collector where the ambient air is preheated, the drying chamber where the material to be dried comes in direct contact with the hot air from the collector and reduces its moisture, and connecting ducts.

2.4.1 Solar Collector

The solar collector plays the part of primary energy source for a solar dryer. Essentially it has functions of energy conversion and energy transfer. The prediction of the solar collector performance requires information on the solar energy absorbed by the collector absorber

plate. The solar energy incident on a tilted surface has three different components: beam radiation, diffuse sky radiation, and diffuse ground reflected radiation and on hourly basis the absorbed radiation $, I_T$ [1], is

$$I_T = I_b R_b (\tau\alpha)_b + I_d (\tau\alpha)_d \frac{(1+\cos\beta)}{2} + \rho_g (I_b + I_d)(\tau\alpha)_g \frac{(1-\cos\beta)}{2} \qquad 2.1$$

where $\frac{1+\cos\beta}{2}$ and $\frac{1-\cos\beta}{2}$ are the view factors from the collector to the sky and from the collector to the ground, respectively. The subscripts b, d and g represent beam, diffuse, and ground, respectively. The meaning of the angles in Eq. (2.1) is described in Figure 2.10 which shows the relationship between the angles which describe the position of a surface on the earth and the position of the sun, relative to the earth and the surface.

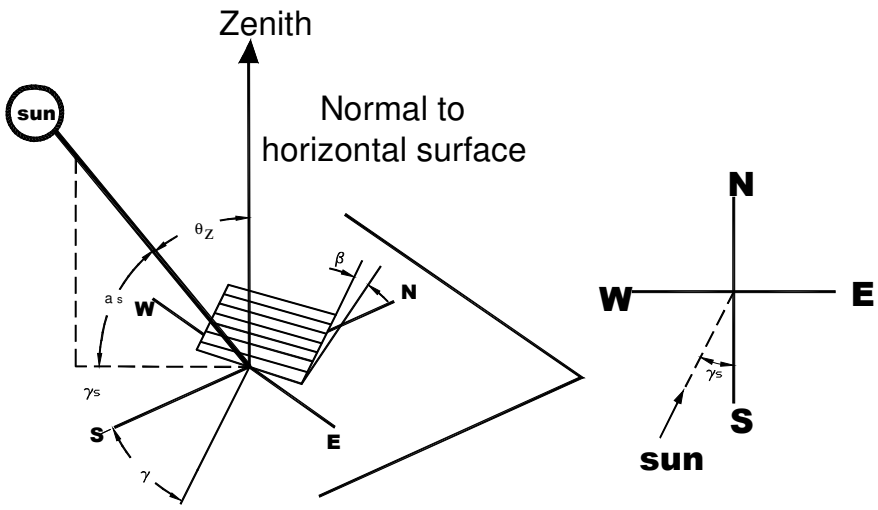

Figure 2.10 Angles describing the direction of a direct solar beam.

[1] The formulae given in this chapter are taken from by Duffie and Beckman (1991) if not stated otherwise.

The symbols have the following definitions:

ϕ Latitude (north positive), $-90^o \le \phi \le 90^o$

β Slope between the plane of the surface and the horizontal, $0^o \le \beta \le 180^0$

γ Surface azimuth angle, $-180^o \le \gamma \le 180^o$

δ Declination.

α_s Solar altitude angle.

θ_z Zenith angle.

The declination angle may be found using the equation:

$$\delta = 23.45 \sin\left[\frac{360}{365}(284+n)\right] \qquad 2.2$$

where n is the day of the year. The following equation relates the angle of incidence to the other angles:

$$\begin{aligned}\cos\theta = &\sin\delta\sin\phi\cos\beta - \sin\delta\cos\phi\sin\beta\cos\gamma \\ &+\cos\delta\cos\phi\cos\beta\cos\omega + \cos\delta\sin\phi\sin\beta\cos\gamma\cos\omega \\ &+\cos\delta\sin\beta\sin\gamma\sin\omega\end{aligned} \qquad 2.3$$

The cross-section of the collector used in this research work is shown in Figure 2.11. The flow of air is under the absorber to reduce the convective heat loss of the air from the covering. The channel depth is 80 mm.

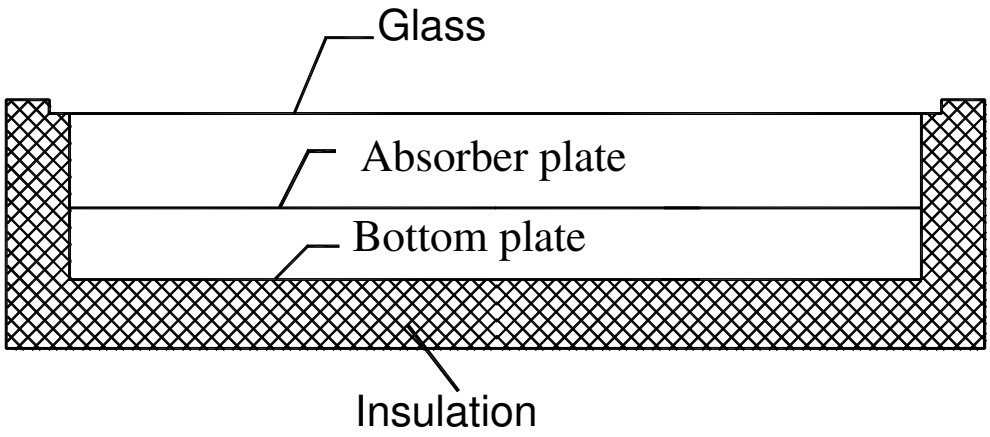

Figure 2.11 Cross section the solar dryer flat plate collector.

It is convenient to define an average transmittance-absorbtance as the ratio of the absorbed solar radiation, S, to the incident solar radiation, I_T.

Thus,

$$S = (\tau\alpha)_{ave} I_T \qquad 2.4$$

This is especially convenient when direct measurements are available for I_T.

2.4.2 Transmittance and Absorbtance

When radiation is incident on the cover of a collector, most of the radiation is transmitted through the cover, and some reflected back. The transmitted radiation easier absorbed by the absorber or reflected back to the cover. Figure 2.12 demonstrates the situation, where τ is the transmittance of the cover system at the desired angle and α is the angular absorbtance of the plate. The product $(\tau\alpha)$ should be thought as symbol representing a property of the cover-absorber combination [9].

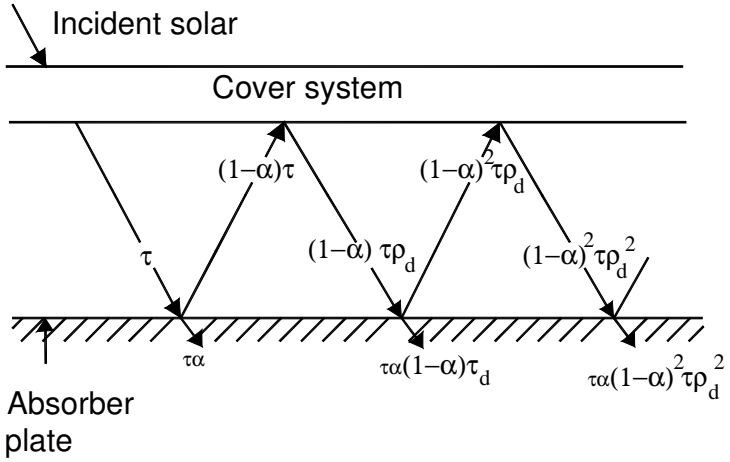

Figure 2.12 Absorption of solar radiation by absorber plate under a cover system

The fraction of energy absorbed after all the reflection is given as:

$$(\tau\alpha) = \tau\alpha\sum_{n=0}^{\infty}[(1-\alpha)\rho_d]^n = \frac{\tau\alpha}{1-(1-\alpha)\rho_d} \qquad 2.5$$

where ρ_d refers to the reflectance of the cover system for diffuse radiation incident on the bottom side, and α the absorptance of the absorber plate.

2.5 Drying Efficiencies

The efficiency of solar drying can be studied under two contexts: Collection efficiency (η_c) and the system efficiency (η_s) [20].

Collection efficiency (η_c) measures how effectively the incident energy on the solar collector is transferred to the air flowing through the collector and is given as the ratio of the useful energy output (over a specified time period), to the total radiation energy, I_T, available during the same period:

The thermal performance of the solar collector is determined by obtaining values of instantaneous efficiency using the measured values of incident radiation, ambient temperature, and inlet air temperature. This requires continuous measurement of incident solar radiation on the solar collector as well as the rate of energy addition to the air as it passes through the collector, all under steady state or quasi-steady state conditions [13].

$$\eta = \frac{Q_u}{A_c I_T} \tag{2.6}$$

where A_c is the collector surface area. Eq. (2.6) can be interpreted only as a transient value owing to the time dependence of the irradiance.

For definite period, the long-term efficiency of the collector can be expressed with the time integral of utilized and input energy flow rates [13]

$$\eta_c = \frac{\int_0^t Q_u dt}{A_c \int_0^t I_T dt} \tag{2.7}$$

2.5.1 System Drying Efficiency

The system drying efficiency (η_s) or system efficiency is the ratio of the energy required to evaporate the moisture of the commodity to the heat supplied to the drier [20]. Therefore,

$$\eta_s = \frac{w.L}{I_T \cdot A_c} \tag{2.8}$$

where, w is the mass of moisture evaporated

L is the latent heat of evaporation of water at the dryer temperature

A_c is the solar collector area.

and the dryer efficiency is given by

$$\eta_d = \eta_s / \eta_c$$

2.5.2 Calculation of Collector Efficiency

In Eq. (2.6) of the instantaneous efficiency, utilized heat flow rate Q_u is the difference between the heat flow rate absorbed Q_a and the heat flow rate lost Q_l to the ambient air:

$$Q_u = Q_a - Q_l \tag{2.9}$$

where

$$Q_a = \tau\alpha I_T A_c \tag{2.10}$$

is the heat flow rate absorbed by the absorber from the irradiation getting through the covering, and

$$Q_l = A_c U_L (T_p - T_a) \tag{2.11}$$

is the heat flow rate transferred to the ambient air from an absorber at temperature T_p. In Eq. (2.11), U_L is the overall heat transfer coefficient of the collector to the ambient air. Substituting into Eq. (2.6) the instantaneous efficiency of the collector is

$$\eta = \tau\alpha - U_L(\frac{T_p - T_a}{I_T}) \tag{2.12}$$

If τ, α and U_L are taken as constant values, instantaneous efficiency in the function

$$f = \frac{T_p - T_a}{I_T}$$

(efficiency function , an independent variable) can be plotted as shown in Figure 2.13. At a given operating point, the utilized energy flow rate from the collector is $Q_u = \eta A_c I_T$.

These considerations can be appropriately applied according to Eq. (2.7) for expressing the long-term efficiency by substituting time averages $(I_T)_{av}$,$(T_p)_{av}$, and $(T_a)_{av}$:

$$\eta = \tau\alpha - U_l(\frac{(T_p)_{av} - (T_a)_{av}}{(I_T)_{av}}) \tag{2.13}$$

From Eqs. (2.12) and (2.13) the threshold value of incident radiation flux can be determined with which the absorbed energy flow rate and loss heat flow rate equal and thus the efficiency is zero:

$$I_{th} = \frac{U_l[(T_p)_{av} - (T_a)_{av}]}{\tau\alpha} \qquad 2.14$$

From I_{th}, using the appropriate metrological data, the possible operation time of the correlation can be stated.

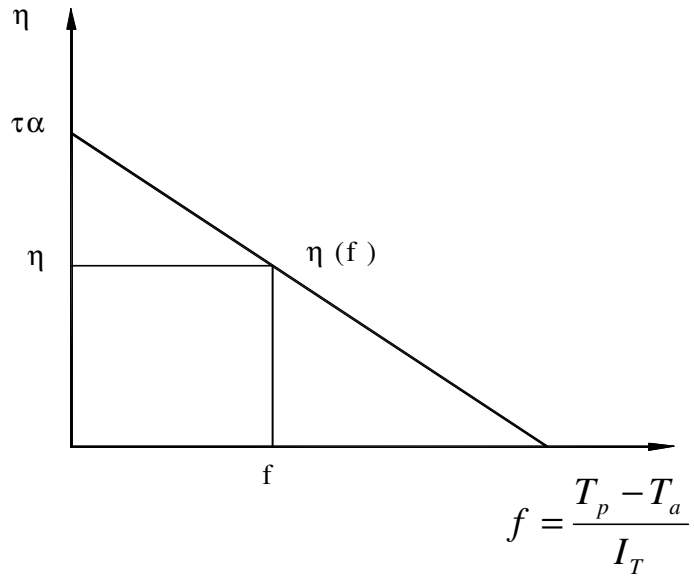

Figure 2.13 Instantaneous efficiency diagram of a flat-plate collector

The instantaneous efficiency of a collector can also be expressed from the known inlet temperature T_{in} of the working medium with the aid of the heat removal factor $F_{R.}$ Since the collector works as an open cycle, drawing external air, a configuration often utilized for air heaters only, the inlet temperature coincides with the environmental one: $T_i = T_a$. Under this working condition the following is used to calculate the efficiency of the collector [17].

$$\eta = F_R\left[(\tau\alpha)_e - \frac{U_L(T_o - T_a)}{I_T}\right] \quad 2.15$$

Where F_R is the factor of heat removal referred to the outlet air temperature and can be expressed as

$$F_R = \dot{m}C_p[\exp(U_L F'/GC_p) - 1]/U_L A_c \quad 2.16$$

where $G = \frac{\dot{m}}{A_c}$

Further, instantaneous efficiency can be expressed directly as a ratio of useful heat flow rate coming into the working medium heat flow rate on the absorber:

$$\eta = \frac{\dot{m}C_p(T_{c,out} - T_{c,in})}{A_c I_T} \quad 2.17$$

Where, $\dot{m}$ is the mass flow rate of air through collector and is given by

$$\dot{m} = \rho .\mathrm{Q} \quad 2.18$$

ρ is density of air

Q is volume flow rate of air

C_p is specific heat of air

In practice, η versus $(T_{in} - T_o)$ or η versus $(T_{c,out} - T_{c,in})$ diagrams are used in place of the η versus (f) efficiency diagram. For representation of the thermal behavior of collectors, besides those above, other practical diagrams, such as η versus $(T_{c,in})$ and η versus $(T_{c,in})$, function curves, can also be used. In these cases other factors in the η equation appear as the parameters of the efficiency curves.

The simplified calculation method has several weak points. One is that the value of T_p must be known to perform the calculation. The temperature of the absorber plate changes in the flow direction of the working medium, and T_p can be interpreted only as a mean temperature.

The greatest error appears in the application of the overall heat transfer coefficient U_L and its use as a constant value. U_L models the overall effect of complex and nonlinear heat transfer processes. Its value for a given collector depends on the local values of T_p, on the sky temperature T_s in view of radiation, on the mass flow rate of the working medium, and on the weather (e.g., wind) conditions. In the value of U_L, the temperature dependence of the heat transfer from the covering is strong. One can interpret the value of U_L as cumulative effects of three coefficients: heat transfer from top covering (U_t), from the bottom plate (U_b), and from the edges (U_e):

$$U_L = U_t + U_b + U_e \tag{2.19}$$

where, the top heat transfer coefficient from the absorber plate to the ambient, U_t, by convection and radiation empirical equation is given by Klein 1975 [24]:

$$U_t = \left\{ \frac{N}{\frac{C}{T_p}\left[\frac{T_p - T_a}{(N+f)}\right]^{0.33}} + \frac{1}{h_w} \right\}^{-1} + \frac{\sigma(T_p + T_a)(T^2{}_p + T^2{}_a)}{[\varepsilon_p + 0.05\,N(1-\varepsilon_p)]^{-1} + \frac{2N+f-1}{\varepsilon_g} - N} \quad (W/m^2K) \tag{2.20}$$

where N = number of glass covers $1 \le N \le 3$

$$f = (1 + 0.04h_w + 0.0005h_w{}^2)(1 + 0.091N) \tag{2.21}$$

$$C = 365.9(1 - 0.00883\beta + 0.0001298\beta^2) \quad 0^0 \le \beta \le 90^0 \qquad 2.22$$

$\beta =$ collector tilt (degrees)

$\varepsilon_g =$ emittance of glass

$\varepsilon_p =$ emittance of plate $0.1 \le \varepsilon_p \le 0.95$

$T_a =$ ambient temperature $260 \le T_a \le 310K$

$T_p =$ mean plate temperature $320 \le T_a \le 420K$

$h_w =$ wind heat transfer coefficient (W/m^2 ^{o}C) $0 \le h_w \le 10m\sec^{-1}$

If the wind velocity is $V[m/s]$, then:

$$h_w = 5.7 + 3.8V \qquad 2.23$$

The energy losses through the back of the collector are caused by conduction through the insulation and convection and radiation to the environment. The convection and radiation part may often be assumed to be close to zero and may be neglected. The back loss coefficient may be approximated to

$$U_b = \frac{k_{in}}{L_{in}} \qquad 2.24$$

where k_{in} is the thermal conductivity of the insulation, and L_{in} is the thickness.

The evaluation of the edge loss is complicated. But fortunately the losses are usually small. The losses through edges should be referenced to the collector area. If the edge loss coefficient area product is $(UA)_{edge}$, then the edge loss coefficient , based on the collector area A_c , is

$$U_e = \frac{(UA)_{edge}}{A_c} \qquad 2.25$$

Chapter 3

Experimental Setup and Instrumentation

3.1 Dryer Setup

The solar assisted indirect dryer discussed here, consists of a solar air collector, a drying chamber and appliances. An outlay of the dryer is given Figure 3.1. Outer side black painted steel sheet of 0.8 mm thick and 4 mm thick glass are used for the construction of the chamber body.

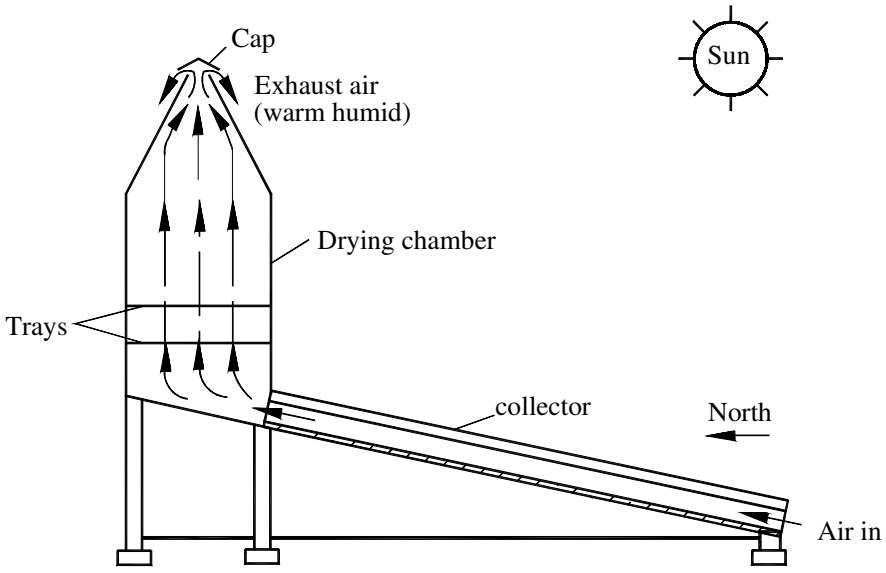

Figure 3.1 Schematic figure of the free convection dryer

The solar collector is parallelpiped shape with dimension of L=2 m x W =1 m x 0.14 m having 80 mm channel depth, 40 mm gap between the absorber plate and glass, and on the bottom 20 mm thick fiber glass insulation. In the present study, its longitudinal axis is oriented along the N–S direction. The collector is inclined at an angle of 12^0 with the horizontal and the optimum angle for latitude of 9^0. The absorber plate consists of 1 mm thick steel flat sheet blackened on the sun facing side. The cover material of the collector is 4 mm thick commercial glass. The lower end face of the collector (1 m x 0.08 m) is the air inlet to the dryer whereas its higher face end is connected to the rectangular duct of the chamber.

The drying chamber is a long rectangular column consisting iron frame with its two sides (the right and the front) covered with glass, the front facing south and the east with a glass door and the rest is covered by sheet metal. Fresh outside air enters through the inlet of the air heater, gets heated during its passage to the air heater. The heated air rises through the drying trays in the drying chamber and leaves the chamber at the top through the exhaust opening. Thus, the material to be dried gets heated directly by absorbing heat through the glass walls and from heated air coming from solar air heater by natural convection.

The drying chamber has 1.2 m x 1.04 m x 0.55 m outer dimensions. Inside the drying chamber three shelves were prepared but only two trays (T1 and T2) were inserted, on which the products to be dried are placed. Each tray is 19 mm deep with wire mesh in the bottom and its area is A_1=0.39 m^2 and A_2= 0.42 m^2, with the two trays in the chamber the total area is 0.81 m^2. The relative positions of these trays are: the bottom tray (tray T1) is

placed 0.18 m above the drying chamber's base (hot air's entry point); the middle tray (tray T2) is located at 0.32 m and the top tray (tray T3) at 0.46 m above the chamber's base, respectively. On the drying chamber, holes were drilled to accommodate rod-shaped measuring probes. The dimensions of the trays are shown in Appendix B of Figure B.2.

3.2 Sensors Positioning

The aim of the research work is experimental performance evaluation of the solar dryer. For this reason, a measuring system is installed in and around the dryer. Figure 3.2 shows the location and types of the sensors applied.

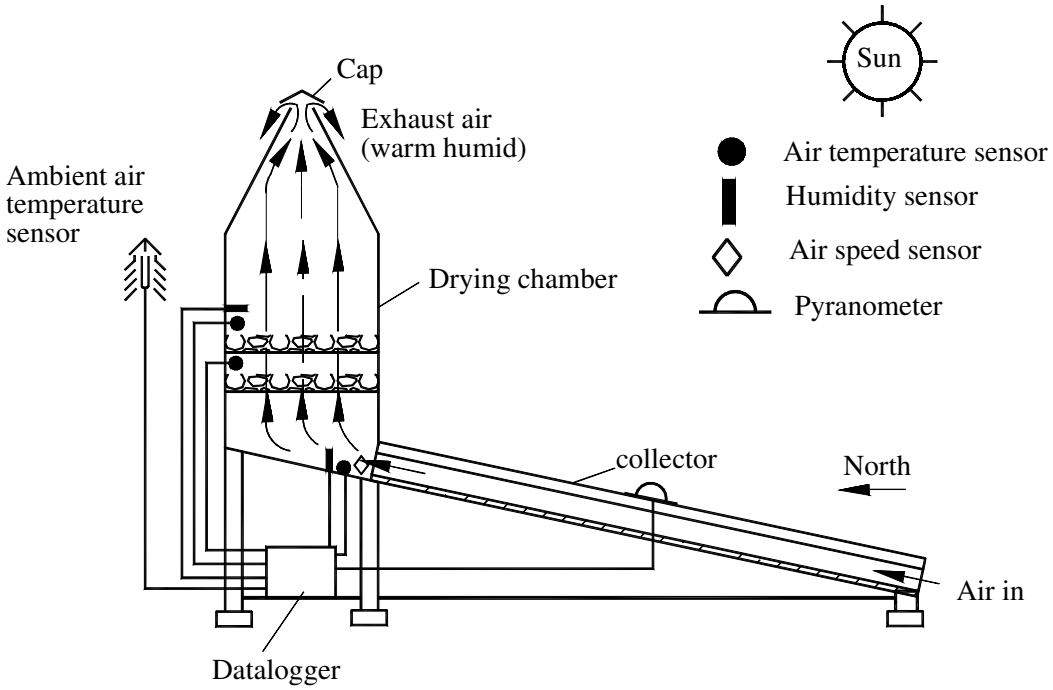

Figure 3.2 Schematic diagram of test set-up

3.3 Instruments

3.3.1 Data Logger

The DL2e logger unit contains all the hardware required for capturing and storing data from a wide variety of sensors, under most environmental conditions. It runs an internal logging program that is set up by the user, and tells the logger how and when to acquire data.

Figure 3.3 Data Logger front panel

3.3.1.1 **Features of** the **Data Logger**

The DL2e Logger is a programmable data logging device, capable of taking readings and storing data from a wide variety of sources. It is independently powered, capable of operating under wet conditions, and at high and low temperatures.

PC software Ls2Win is first used to program the logger, specify what sensors are to be connected to the logger, and how frequently to record data. Once the logger has been set up, the PC can be disconnected and the logger can be left to operate on its own. Data recorded from sensors is stored in the logger's own memory, and periodically transferred to a PC or to any device which has an RS232 serial port, for example a printer. When data has been collected from logger, it can be cleared from the logger's memory to make room for more data.

Only one PC is needed to operate any number of loggers, and it only needs to be connected while setting up the logger and collecting the stored data. The logger also has a front panel with keypad and display that can be used to check and control logger operation without using a PC. The DL2e Logger is modular in design. Depending on the input cards installed, the logger can record data from up to 62 sensors. Input cards are available for analogue and pulse output sensors. Each logger has on board digital input channel for pulse counting or event detection, and two relays, for powering up sensors or simple control applications.

The logger has an internal clock and can be set up to record data at regular intervals. This is known as timed data. In addition, it can also record data when events are detected known as event triggered data.

The logger can be powered from external DC power supply, or from its own internal batteries. It has extremely low power consumption and can operate for extended periods on a set of batteries. With a rugged weatherproof case, it is equally suited for use as a laboratory instrument or for outdoor installation for remote locations. Being modular and

programmable, it is an extremely flexible tool, and easily adaptable for a wide variety of application.

3.3.1.2 Data Logger Software (LS2Win)

Ls2Win enables a PC to communicate with the logger, edit logging programs and collect the data. It is supplied on CD-ROM and the installation procedure is as follows [5].

3.3.1.3 Items Required for Installation of LS2Win

To operate the logger from your PC the following are need:

- A PC running windows 95,98,2000 or NT4.0 Service pack 4, or later.
- One free RS232 serial port.
- CD-ROM drive (required for installation)
- At least 16M RAM memory and 5Mb for hard disk space.
- Logger-PC RS232 cable: Type LRS1 available from Delta-T or you can make up.

Setup installs a program group named Ls2Win on the program menu, which contains the following items:

- *New DL2 Control Panel,* For creating 'DL2 Control Panels' which one can use to communicate with the data logger;
- *DL2 Program Editor,* for creating and viewing logging programs;
- *Dataset Viewer,* for inspecting the contents of 'data set' files (files containing logged data);

- *Dataset Import wizard,* for importing logged data in to Microsoft Excel.

Setup also installs desktop shortcuts that correspond to each item in the Ls2Win program group.

Figure 3.4 A programming group of the Ls2Win software

3.3.1.4 Create a New DL2 Control Panel

Double click the New DL2 control panel desktop icon (or select New DL2 Control panel from the start, programs, Ls2Win menu) this will open the DL2 Control Panel.

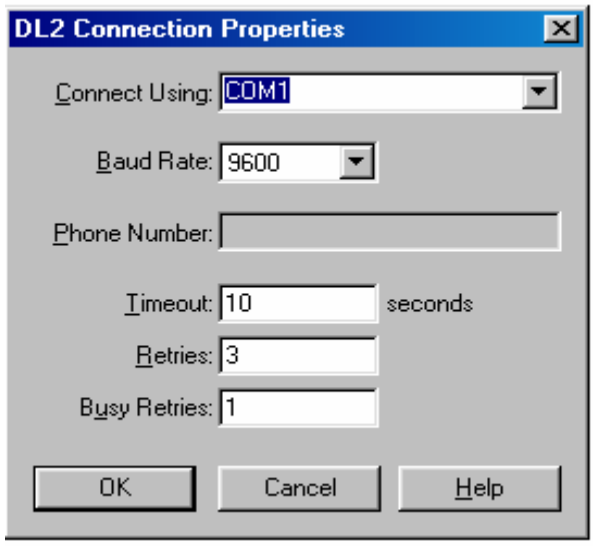

Figure 3.5 Connections properties dialog box

On clicking OK a dialog box appears to save the connection properties as a DL2 control panel file. A Save DL2 control panel dialog box is shown below. Write the file name in this case "dryer" *and click OK* to accept the file name.

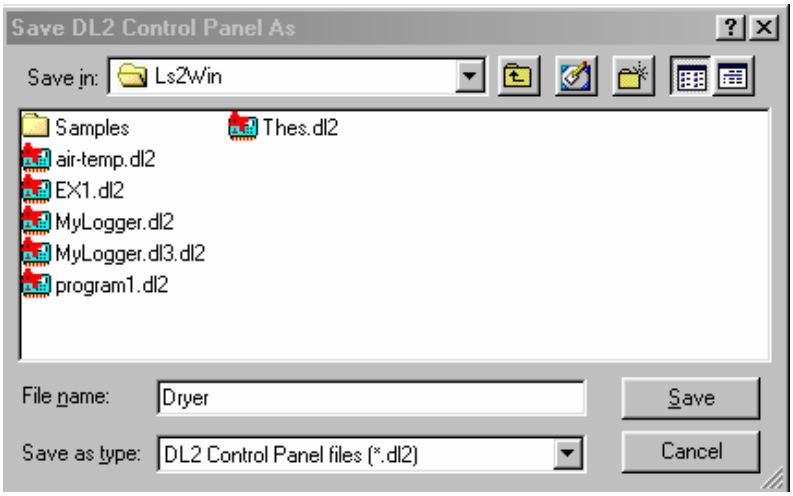

Figure 3.6 Save DL2 control panel dialog box

DL2 control panel now creates a short cut icon to it self on the disk top and retrieves and displays states of information from the logger. You have now established communication with the logger. If you select the incorrect connection setting, select properties from the file menu, change the setting in the DL2 connection properties dialog, and click refresh to refresh DL2 control panel.

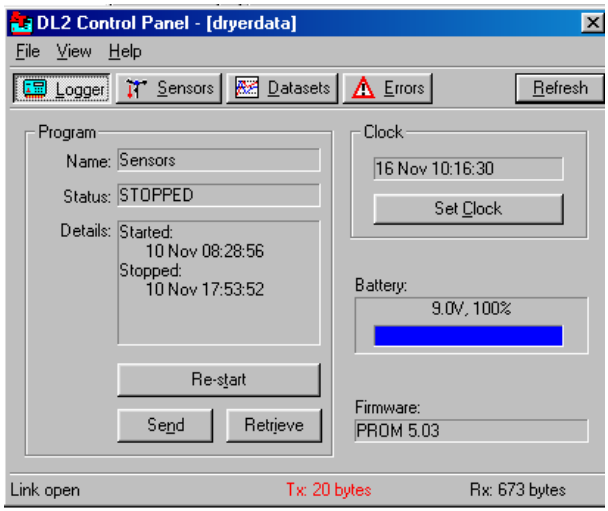

Figure 3.7 Logger Panel on the DL2 Control panel

This figure shows the dialog box of the control panel after communicating with the logger. There are four panels of information in the DL2 control panel: you switch between them by clicking the Logger, Sensors, Datasets and Error buttons. Figure 3.7, Logger-Panel shows the general information about the state of the logger.

3.3.1.5 Logger Panel

It inspects the logger status and start logging. The Program *Name* is the name of the logging program currently stored in the DL2. The program *states* can be:

- *Standing by:* not logging, not logged data
- *Armed:* Awaiting a start trigger, but NOT awaiting first TIMED data
- *Logging:* actively recording data (or awaiting first TIMED data)
- *Stopped:* not logging logged data exists.

3.3.1.6 Sensors Panel

On clicking the sensors tab, it will show Figure 3.8. The sensor panel is used to test whether each connected sensor is working properly or not. Since the reading may be a wrong value therefore each reading should be checked against the expected value. This is useful for inspecting the sensors before logging started. Click *select All and either* Enable *Read continuously* or *Read Now to see the sensor reading*: the display below shows the sensors being read continuously.

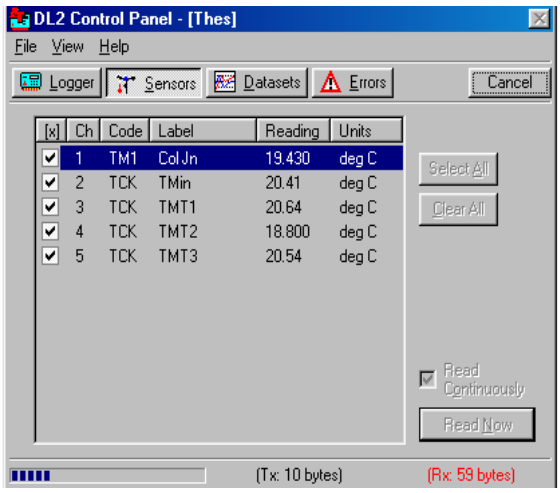

Figure 3.8 Sensors panel showing real time readings from temperature sensors

3.3.1.7 Dataset Panel

It is used to retrieve the dataset. The dataset panel displays the information about readings stored in the logger. Clicking *Datasets* and then *Refresh,* one obtains.

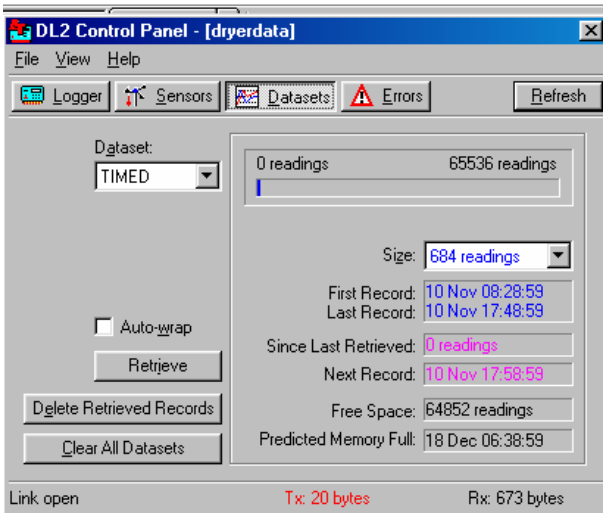

Figure 3.9 Dataset control panel, displaying the information about the readings stored in the DL2

Inspect the dialog; most of the indicated values are self-explanatory.

- *Dataset:* A logger program can generate up to three datasets: the TIMED dataset contains data recorded at regular recording intervals, and TRIG/61 and TRIG/62 datasets which contain data recorded on detection of events on digital input channels 61 and 62 respectively.
- *Auto-warp:* If selected, when memory is full, the most recent data overwrites the oldest readings. The most recent data are retained; the oldest data are overwritten by new data. This option is only available for TIMED dataset.
- *Retrieve*: Retrieves the selected dataset to a PC disk file.
- *Delete retrieved Records:* Delete the most recently retrieved dataset records from the logger's memory. This option is only available for the TIMED dataset. For TRIG/61 and TRIG/62 datasets, the alternative command is *Delete All Records*, which deletes the entire contents of the selected dataset from the logger's memory.
- *Clear All Dataset:* Deletes the contents of all datasets from the logger's memory. This command is only enabled when the logger is not logging.
- *Size:* Determines how used and available memory is played from a large drop down list of options.

3.3.1.8 Programming the DL2e Logger

For real logging applications, a logging program is needed. A logging program specifies some or all of the following:

- What sensor types are connected to each of the logger's channels,
- How frequently readings are to be logged from each channel,
- What type of units the raw readings are converted to,
- When or how logging should start,
- What happens when memory is full,
- How long a sensor shall receives power before taking a reading

3.3.1.9 The DL2 Program Editor

Select the logger panel in the DL2 control panel and click retrieve. The program will appear, laid out as a table in a row of tab sheets, in the DL2 program Editor.

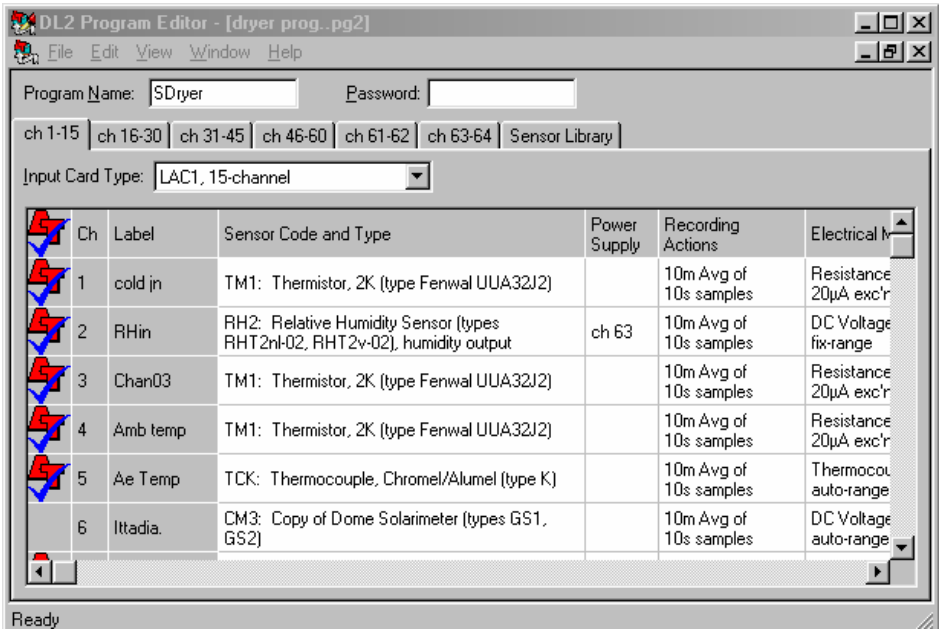

Figure 3.10 A copy of the "dryer"-logging program in the DL2 is retrieved and displayed in the program Editor

3.3.1.10 Retrieving Logged Data to PC

The Ls2Win program called DL2 control panel to:

- Display information about the logger and its datasets
- Display data settings in real-time
- Retrieved logged data from the logger data from the logger to a PC disk file
- Display the data on your PC screen

3.3.1.11 Dataset Viewer

This is a separate program that automatically opens on the desk top when a dataset viewer in the DL2 control panel is retrieved. This shows the reading of the connected sensors from the dryer at different locations at interval of 10 minutes. The binary format dataset is displayed in the dataset viewer.

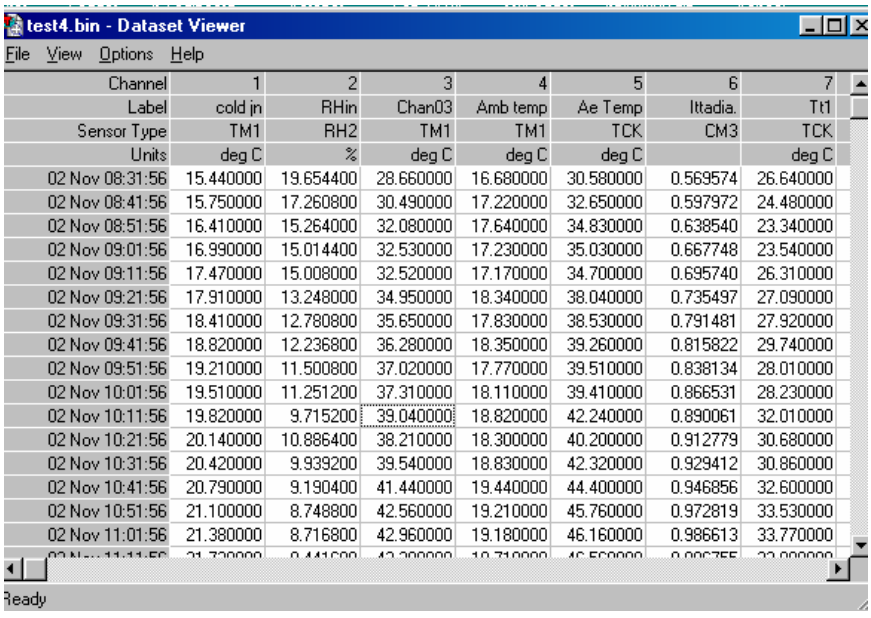

Channel	1	2	3	4	5	6	7
Label	cold jn	RHin	Chan03	Amb temp	Ae Temp	Ittadia.	Tt1
Sensor Type	TM1	RH2	TM1	TM1	TCK	CM3	TCK
Units	deg C	%	deg C	deg C	deg C		deg C
02 Nov 08:31:56	15.440000	19.654400	28.660000	16.680000	30.580000	0.569574	26.640000
02 Nov 08:41:56	15.750000	17.260800	30.490000	17.220000	32.650000	0.597972	24.480000
02 Nov 08:51:56	16.410000	15.264000	32.080000	17.640000	34.830000	0.638540	23.340000
02 Nov 09:01:56	16.990000	15.014400	32.530000	17.230000	35.030000	0.667748	23.540000
02 Nov 09:11:56	17.470000	15.008000	32.520000	17.170000	34.700000	0.695740	26.310000
02 Nov 09:21:56	17.910000	13.248000	34.950000	18.340000	38.040000	0.735497	27.090000
02 Nov 09:31:56	18.410000	12.780800	35.650000	17.830000	38.530000	0.791481	27.920000
02 Nov 09:41:56	18.820000	12.236800	36.280000	18.350000	39.260000	0.815822	29.740000
02 Nov 09:51:56	19.210000	11.500800	37.020000	17.770000	39.510000	0.838134	28.010000
02 Nov 10:01:56	19.510000	11.251200	37.310000	18.110000	39.410000	0.866531	28.230000
02 Nov 10:11:56	19.820000	9.715200	39.040000	18.820000	42.240000	0.890061	32.010000
02 Nov 10:21:56	20.140000	10.886400	38.210000	18.300000	40.200000	0.912779	30.680000
02 Nov 10:31:56	20.420000	9.939200	39.540000	18.830000	42.320000	0.929412	30.860000
02 Nov 10:41:56	20.790000	9.190400	41.440000	19.440000	44.400000	0.946856	32.600000
02 Nov 10:51:56	21.100000	8.748800	42.560000	19.210000	45.760000	0.972819	33.530000
02 Nov 11:01:56	21.380000	8.716800	42.960000	19.180000	46.160000	0.986613	33.770000

Figure 3.11 Dataset retrieved from the logger to file

The dataset viewer is also available as an icon on the desk top. The Dataset Viewer offers the following commands:

Open: Command (file menu) opens and displays a DL2e dataset file.

Save As: command (file menu) saves the dataset, which is currently open in the dataset viewer as a data format file- a comma to separated ASCII format, which is compatible with most data processing applications.

Date Format: Command (View menu) allows you to select the Day/Month order for interpreting ambiguous data file timestamps.

3.3.2 AMB Moisture Balance (AMB 50, AMB 110 and AMB 310)

The AMB moisture balance is a laboratory instrument of the type AMB 310. It is used to determine the initial and final moisture contents of the material to be dried and its measuring capacity is in the range of 4 to 310 g.

The AMB moisture balance is easy to use. The user sets the drying parameters into memory, puts the samples into the weighing chamber and then starts the test. The temperature of drying is automatically regulated and the results: elapsed time, current temperature in the chamber and the mode are displayed during the test. The user is told when the test has automatically stopped either due to the sample being dry and the weight no longer changing, or the elapsed time reaching the limit the user has set. The final values are held on the display until the user resets the balance.

The balance can be interfaced to a printer or computer. The results are shown when the test progresses and after the test has finished a summary of the test can be sent to a PC or printer.

At the end of the test the following data are displayed over the digital displays of the *AMB moisture balance*.

i) Percentage moisture or Percentage Solids

ii) Initial mass [mg]

iii) Final mass [mg]

iv) Drying temperature [^{o}C]

v) Elapsed drying time [s]

vi) Time interval between two successive measurements [s]

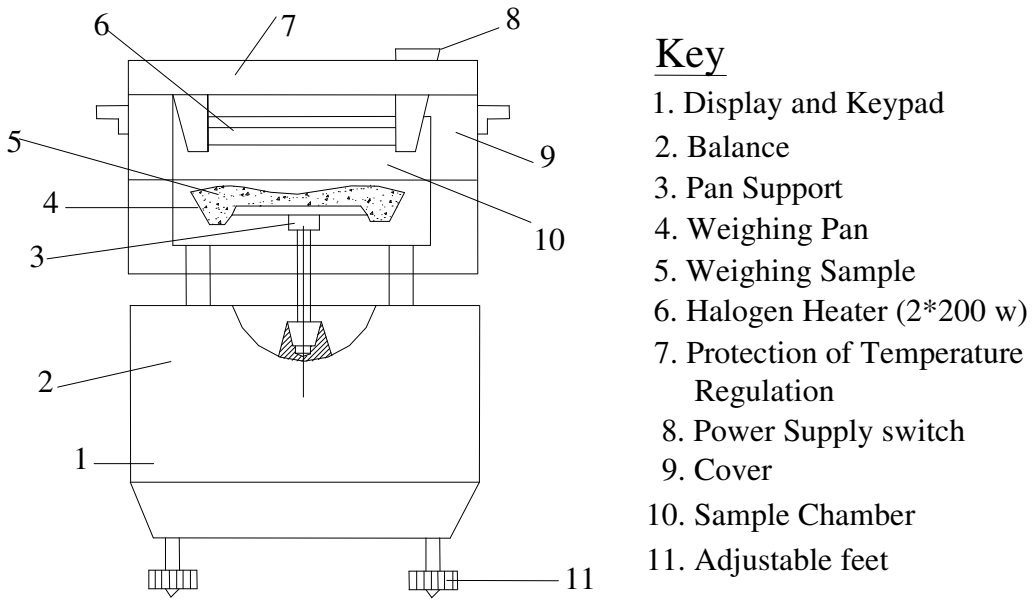

Figure 3.12 AMB moisture balance description

3.3.3 Dome Solarimeter (Pyranometer)

The Global radiation is monitored by Delta-T Device Ltd of type GS1 dome solarimeter. The instrument gives the instantaneous solar irradiance in kW/m^2. The pyranometer model is CM3. Sensitivity temperature deviation (-10 to +40^{o}C) 6% relative to 20^{o}C and its sensitivity 10-35 $\mu V / W.m^{-2}$. The connection of the pyranometer with the data logger is made according to the setting provided by the data logger supplier [3].

3.3.4 Anemometer

The anemometer is a versatile wind speed indicator which can be used wherever an accurate visual reading of wind speed is required. The anemometer used is of type digital anemometer from Delta-T Device Ltd. It measures flow velocities in the interval $0\ to\ 250\ m/s$ .The display accuracy is 1 degree and sensor accuracy is 0.5 degree.

3.3.5 Ambient Air Temperature Sensor

The temperature sensor used is of type AT2-052 a thermistr from Delta-T Device Ltd. It measures ambient temperature in the range of $-50\ to 150^{0}C$. It has an accuracy of $\pm 0.1^{0}C$

3.3.6 Air Temperature Sensor

The common features of AT2 air temperature sensor is the solar radiation shield that protects the sensors from solar radiation and rain when they are mounted outdoors. The temperature sensors used to measure air inside the drying is of K type thermocouple from Delta-T Device Ltd. It measures temperature in the range of $-120\ to 200^{0}C$ with an accuracy of $\pm 0.1^{0}C$ [6].

3.3.7 Humidity Sensor

To measure relative humidity, sensors from Delta-T Device Ltd of type RHT2nl-02, are used. The accuracy at 23^{0}C is $\pm 2\%\ RH\ (5\ to\ 95\%\ RH)\ \pm 2.5\%\ RH\ (RH < 5\ and > 95\%)$ [6].

3.3.8 Hot Wire Anemometer

Air velocity is measured by hotr wire anemometer, NTC anemometer from Testo instruments. It measures flow velocities in the interval $0\ to\ 20\,m/s$. The accuracy is within $\pm 0.05\ m/s \pm 5\%\ \ of\ m.v\,(0\ to\ 2\,m/s)$ and $\pm 0.5\ m/s \pm 5\%\ \ of\ m.v\,(2\ to\ 20\,m/s)$.

3.3.9 A Digital Platform Balance

It is used to determine the weight loss of the dried product within the specified time interval. The accuracy is within $\pm 0.1g$.

3.4 Program Installed in the Data Logger

First, the program is prepared on the PC and later transferred to the logger via RS232 serial port. DL2e programming editor is used to retrieve some of the sensors and adapt others from the DL2e library. After configuring the each channel, the recording action is set to 10 minutes. The name of the program used for the data collection is SDryer, which is shown in Figure 3.13.

In the program the following terms are used for the name of the sensors

Label	Description
Cold jn	Cold junction temperature in the data logger
Amb temp	Ambient temperature
Irradia	Solar radiation at the surface of the collector
Ae temp	Air outlet temperature from the collector

Tr1 temp	Air temperature over tray 1
Tr2 temp	Air temperature over tray 2
Tr3 temp	Air temperature over tray 3
Tto	Temperature at the exit of the dryer chamber
RH in	Humidity of air inlet to the chamber
RH out	Humidity of air out from the chamber

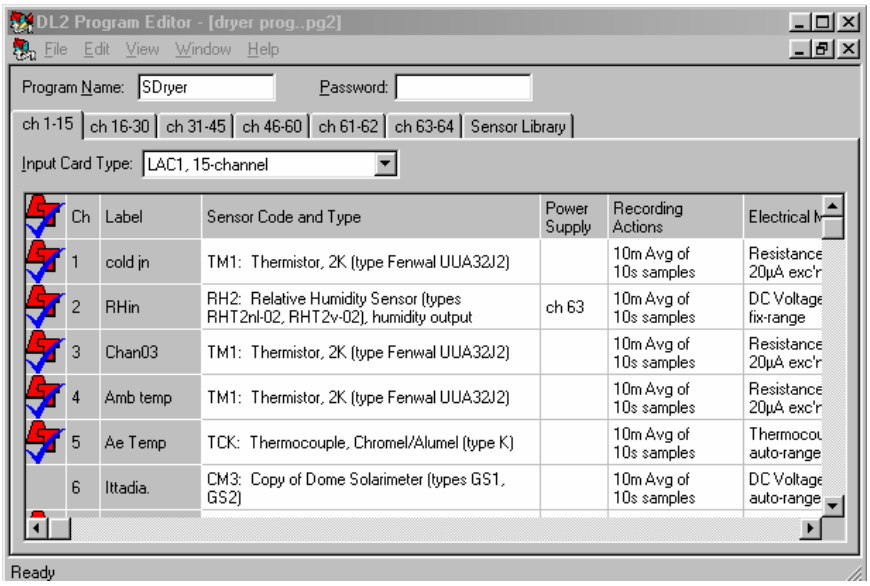

Figure 3.13 A copy of the logging program used in this project.

Chapter 4
Test Procedure and Computations

4.1 Sample Preparation

Before the test was conducted with material to be dried, the dryer was checked with no load. The exit and inlet flow areas were reduced by closing the air flow channels at the expense of the air flow rate until a drying air temperature above 38^{o}C was achieved which is required for the drying of fruits and vegetables [16].

The important factors affecting the migration of moisture from the interior of a particle to its surface are the temperature of the particle, its moisture content, the physical dimensions, the internal structure and the composition of the material.

The change in moisture content with time is proportional to the change in moisture gradient across the particle from the interior to the surface. In other words, the rate of drying decreases with decrease in moisture content but increases with decrease in particle size. Therefore, the potato was washed repeatedly until it was clean and then sliced using a manual slicing machine to increase the rate of drying.

4.1.1 Characteristics of Potato Used in the Experiment

For determination of the average characteristics of the potato, 10 sliced potatoes were taken.

Table 4.1 Characteristics of fresh potato ready for drying purpose

Characteristics	Average Value of potato tested
Shape	Rectangular
Potato weight per tray [kg]	T_1 = 2.45 T_2 = 2.61 T_3 = 2.81
Potato weight per unit area [kg/m^2]	6.21
Potato slice length [mm]	49.8
Potato slice height[mm]	10
Potato slice width [mm]	7
Surface area [cm^2]	18.3
Average weight of each sliced potato [g]	3.3
Average volume of each sliced potato[cm^3]	3.48
Average density [g/cm^3]	0.947
Moisture content potato slice (wet basis) [%]	81.56
Moisture content potato slice (dry basis) [%]	442.3
Moisture content of dried material of the potato slice (wet basis) [%]	2.6-3.6
Moisture content of dried material of the potato slice (dry basis) [%]	2.7-3.73

4.2 Moisture Determination

The initial moisture content on wet and dry basis of the potato used in the experimental work was determined by AMB (AMB 310) moisture balance. The AMB balance test was set at Mode 1, with strobe time interval of 2 seconds and drying temperature 160^0C. Then, slices of potatoes samples were placed on the AMB moisture balance tray. Samples of the potato of weight (w_0) were dried in the moisture balance at 160^0C until the weight (w_d) of the dried sample became stable. The moisture content on wet basis of the potato used was 81.56 % (442.3 % moisture content at dry basis). The moisture content, dry basis, (Md_o) of the potato is expressed as [2]:

$$Md_o = \frac{w_o - w_d}{w_d} * 100 \qquad (\%) \tag{4.1}$$

For the determination of the moisture content, dry basis, (Md_i) of the potato at any time (t_i) during the drying process, the following equation can be used:

$$Md_i = \frac{w_i - w_d}{w_d} * 100 \qquad (\%) \tag{4.2}$$

or moisture content , wet basis, of the potato at any time (t_i) during the drying process

$$Mw_i = \frac{w_i - w_d}{w_o} * 100 \qquad (\%) \tag{4.3}$$

where w_i is the weight of the potato at time t_i

The moisture content on dry basis and wet basis are related by Eq. (4.4) [2]

$$Md = \frac{Mw}{100 - Mw} * (100) \qquad (\%) \tag{4.4}$$

The determination of the potato weight was done by weighing the drying tray with its load of potato at any time in the drying process.

For the determination of the instantaneous drying rate (RDd_i) (dry basis), equation (4.5) was applied:

$$RDd_i = \frac{\Delta w_i}{w_d * \Delta t} = \frac{w_{i-1} - w_i}{w_d * (t_{i-1} - t_i)} \qquad (kg_w / kg_d . \min) \tag{4.5}$$

where t_{i-1} *and* t_i are successive times corresponding to when two successive measurements of a drying material is made and $Md[\%]$.

Another equation can be used for the determination of the drying rate, (dry basis):

$$RDd_i = \frac{Md_{i-1} - Md_i}{100 * \Delta t} = \frac{Md_{i-1} - Md_i}{100 * (t_{i-1} - t_i)} \qquad (kg_w / kg_d . \min) \tag{4.6}$$

The final mass is determined as follows

Final mass=Initial mass x (1- initial moisture content wet basis,w.b.)

4.3 Procedure of the Test

The first step was weighing of empty trays and 2.45kg, 2.61 and 2.81kg sliced potato (equal 6.21 kg/m^2 on each tray) were uniformly loaded and spread over T1, T2, and T3 respectively to form a layer. Then T1 and T2 were placed in the drying chamber and T3 control sample was left to the open sun and dried under natural conditions in the sun. The next step was to check whether the data logger functions properly or not. “Wake” the logger and see the status report, like power supply level, installed program and the functionality of each channel. The power supply level of the data logger should be greater

than 7%. This could be done by adjusting the power output lobe of the adapter to the required value. If the status report is the required one, press wake and then start to begin logging.

The mass of the trays with the potato were recorded every 30 minutes. The potato slices were manually stirred randomly. This would help to increase the temperature of potato slices' and would ease the moisture diffusion through the potato slices. The drying process was considered to be complete once the moisture content of the slices dropped to about 3.1% on wet basis.

Once the solar drying experiment was completed, samples of the solar dried potato were compared with the potato that was dried by open sun. The factor considered in this comparison was drying time.

The measured data from the collector and dryer: air temperature at the outlet of the collector and over trays T1 and T2, relative humidity at the inlet and exit of the chamber, solar irradiance and ambient temperature were also recorded in the data logger at intervals of 10 minutes. The data were scanned each 10 seconds and averaged for 10 minutes. The values were stored in the data logger and by the end of the tests transferred to a personal computer.

4.4 Efficiency Analysis

The efficiency of the dryer is considered by taking into account the complete collector-drier system for the solar energy input. The measured values by the data loggers transformed into

physical meaningful values like solar radiation, temperatures, humidity, air speed and weight.

The useful heat is then estimated from the formula

$$Q_u = \dot{m} c_{pa} (T_0 - T_a) \tag{4.7}$$

where T_0 = Air temperature at exit of collector

T_a = Air temperature at inlet of collector equal to the ambient temperature

Measuring the collector flow exit area, the flow velocity of air, and the local density of the air, the mass flow rate is calculated as

$$\dot{m} = \rho A V \tag{4.8}$$

The instantaneous efficiency of the collector is the calculated from the relation

$$\eta_c = \frac{Q_u}{A_c I_T} \tag{4.9}$$

The cumulative efficiency is calculated from the ratio of the sum of the useful heat and the solar radiation reaching the area

$$\eta_c = \frac{\sum Q_u}{\sum A_c I_T} \tag{4.10}$$

The system drying efficiency (η_s) or system efficiency is calculated from the ratio of the energy required to evaporate the moisture of the commodity to the heat supplied to the drier

$$\eta_s = \frac{w.L}{I_T \cdot A_c} \tag{4.11}$$

where w is the mass of moisture evaporated

L is the latent heat of evaporation of water at the dryer temperature

Chapter 5

Results and Discussion

Four successful tests were conducted between October 11 and November 3, 2004 and in this thesis work one of the test data was used to evaluate the collector efficiency, drying curves, humidity and temperature measurements in the dryer. During the tests period, the heated air was used to dry potato. The test raw data from the experiment is tabulated in the appendix A.

5.1 Collector Performance

5.1.1 Collector Efficiency

The efficiency of the collector could be seen from difference in temperature of the exit and inlet of the air to the solar collector. In this dryer, by fully opening the inlet and the exit of the dryer, a temperature within 10-20^{o}C higher than the ambient air temperature was recorded. However, for drying of the potato the temperature was increased by decreasing the inlet of the collector and outlet of the drier areas and a temperature within 14-29^{o}C higher than the ambient air temperature was obtained and this variation is shown in Figure 5.1.

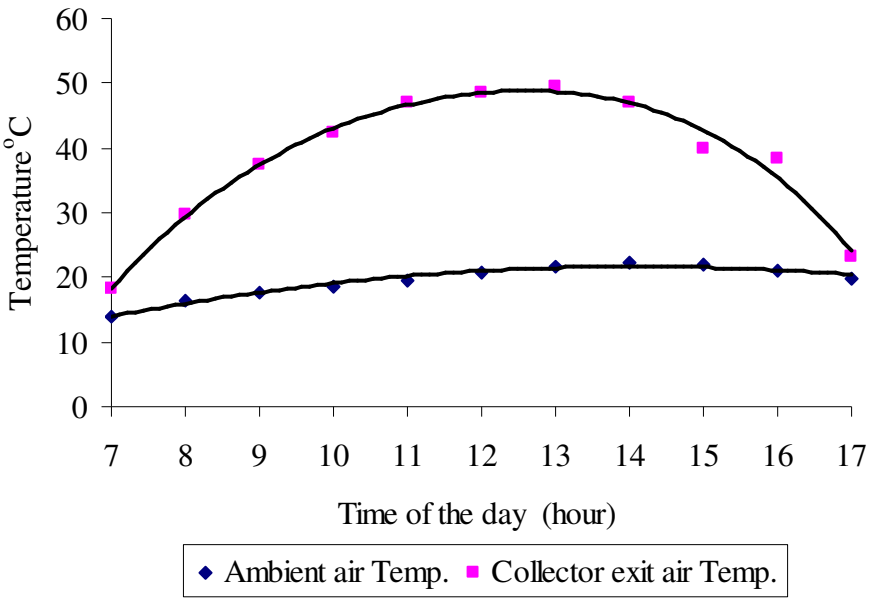

Figure 5.1 Shows the inlet and outlet air temperatures for the collector.

The instantaneous efficiency of the solar collector started to rise in the morning period and was relatively constant at 28.56% from 11: 15 hours to 13:45 hours and dropped down in late afternoon. The variation obtained is typical for a flat plate collector and indicates strong dependence of efficiency on the metrological data. The daily efficiency, averaged over 9 hours (8:30 to 17:30) comes out to be 25.6%.

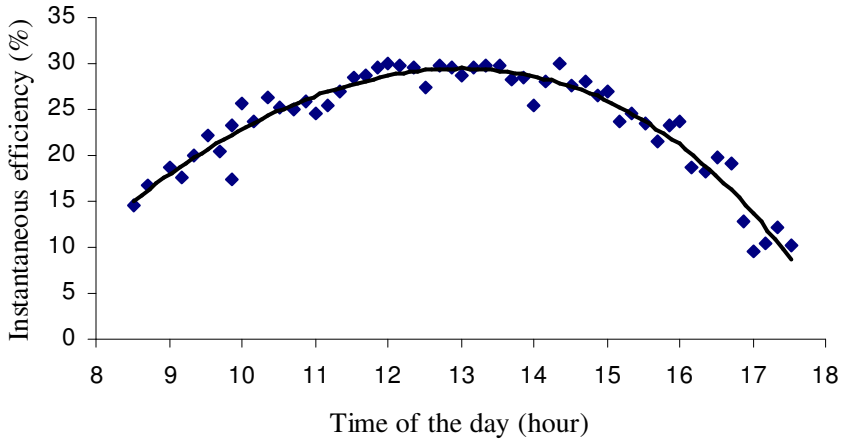

Figure 5.2 Variation of instantaneous efficiency of the flat plate collector.

Figure 5.3 shows a plot of the collector efficiency as a function of the normalized temperature rise $(T_o-T_a)/I_T$. As seen, the collector efficiency curve complies with the standard curve [9].

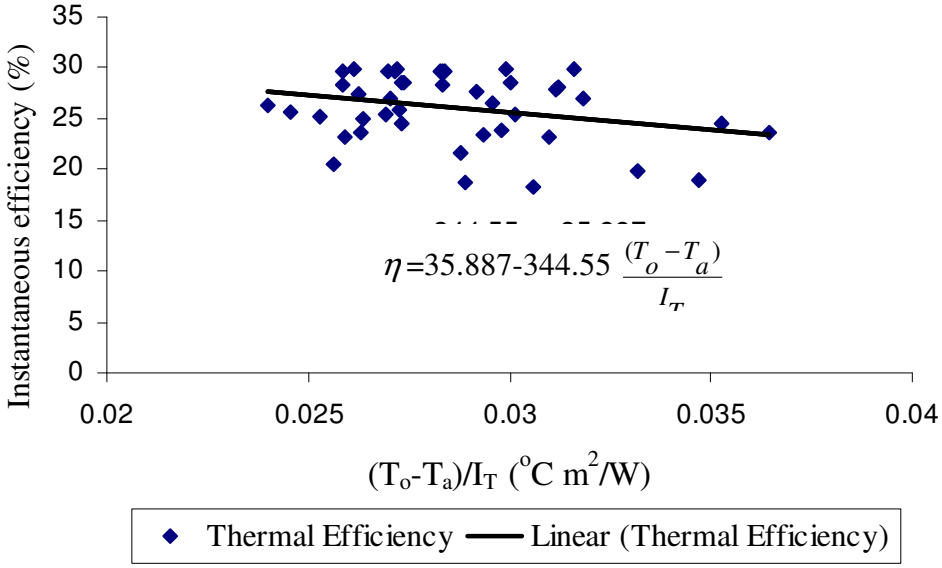

Figure 5.3 Collector Instantaneous efficiency

The plot is made with the beam radiation nearly normal to the collector so that the transmittance-absorptance product for the tests condition is approximately the normal incidence value of the normal incident angle. It was seen that the data points were scattered around the linear fit line. This is because of the fact that during the tests the wind speed was not constant. For the data, the straight line that best approximates them is given by the following equation with correlation coefficient -0.29 :

$$\eta=35.887-344.55\frac{(T_o-T_a)}{I_T} \qquad 5.1$$

In equation (5.1) η is the efficiency. The first term on the right is equivalent to the efficiency when there is no heat loss, and the second term represents the heat loss coefficient..

5.2 Relative Humidity and Capacity of the Air

The relative humidity is affected by the air temperature. Heating the air decreases the relative humidity and respectively increases the capacity of the air to carry away moisture during a drying process. The extent to which this is achieved depends on the weather conditions, namely the absolute humidity and the temperature of the ambient air. The relative humidity and temperature of the ambient air are included for comparison.

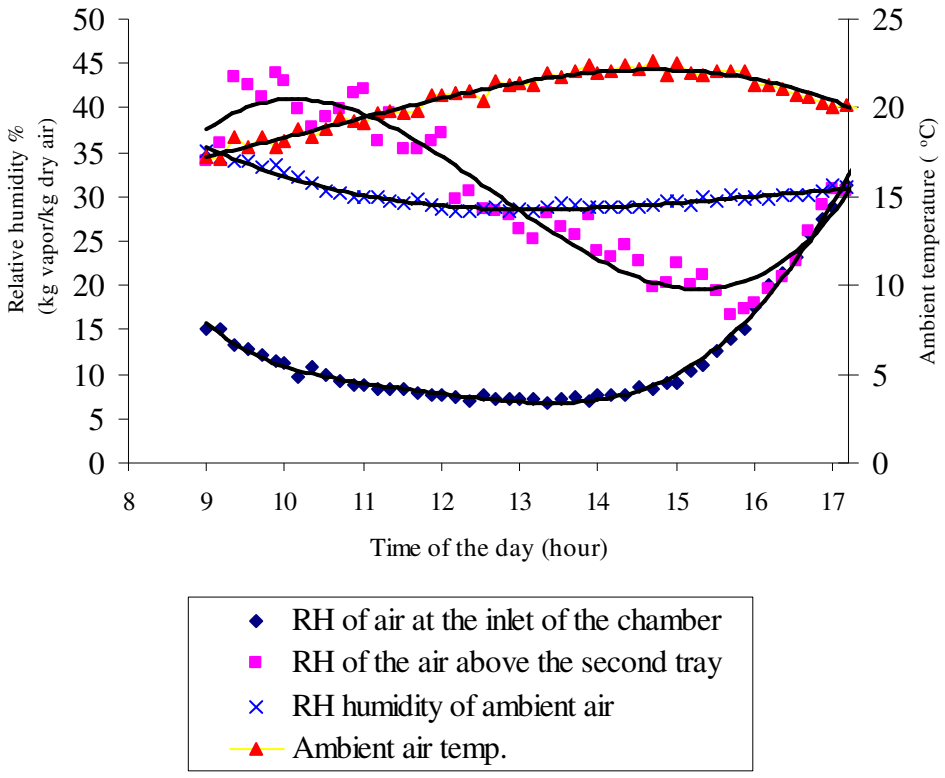

Figure 5.4 Time variation of the relative humidity in the dryer: at the exit of the collector, and just above the second tray.

The average relative humidity of the ambient air was 30.41% compared to the relative humidity of the air at the collector exit which has an average of 11.89% in the morning, 8.7% - 8.9% between 11- 15 hours with a minimum of 6.6% at 13:30 hour and an average of 18.97% in the late afternoon. However, the low relative humidity of the exhaust air shows that the potential of the drying air to remove moisture was not fully utilized this can be seen from the graph in the after-noon. This can be improved through proper utilization of the drying potential of the air by increasing the number of the drying trays.

5.3 Drying Tests

The experimental results obtained are shown in Figures 5.5, 5.6 and 5.7. Figure 5.5 shows the moisture content of potato as a function of the drying time. As may be expected, tray T1, (the one placed nearer to the hot air), exhibits the most rapid drying. By 6 PM of the first day, the moisture content dropped to about 4.37551, 7.881226, and 11.48754% (wet basis) for the potato in the first (bottom), second and open sun tray respectively. During the second day the moisture content decreased gradually. By 10 AM of this day the moisture content dropped to about 2.62, 3.05 and 5.6%. The final moisture contents at 1PM were 2.62, 2.93 and 3.58% on wet basis and which are considered as the equilibrium moisture contents of potato. These moisture contents indicate that the first tray reached the equilibrium moisture content at the end of the first day. The potato in the open sun tray reached equilibrium moisture content after seven hours of the second drying day. This means a reduction of the drying period of 3 to 4 hours was obtained using the solar dryer

compared to the traditional sun drying, depending on the weather conditions. Other advantages are the protection against sunshine, dust, and insects.

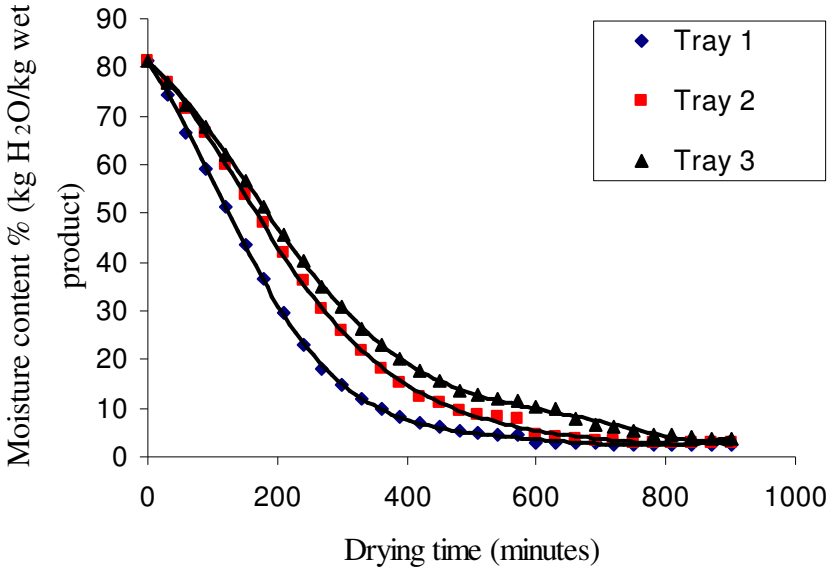

Figure 5.5 Moisture content curves for potato in solar dryer and open air sun dryer.

During the night times the inlet and the exit of the dryer were closed and the control sample was placed in room to prevent the potato from moisture regain. The sudden drop on Figure 5.5 shows there was moisture loss during the night. This is because during the night there was loss of moisture to the air in the dryer and in the room.

Figure 5.6 shows the drying rate of potato as a function of the drying time. As seen from the curves in the figure, the drying rate for the first tray at the bottom of the drying chamber expectedly has the highest drying rate during the first 3 hours. However, as it gets dried its

drying rate decreases. The drying rate of the potato on the second tray is larger than the first one after hours because the drying air absorbs less moisture from the first tray. Even though there was moisture loss during the night in all the trays but the drying rates were nearly zero this is because the moisture loss was the entire night. This effect is reflected in Figure 5.6.

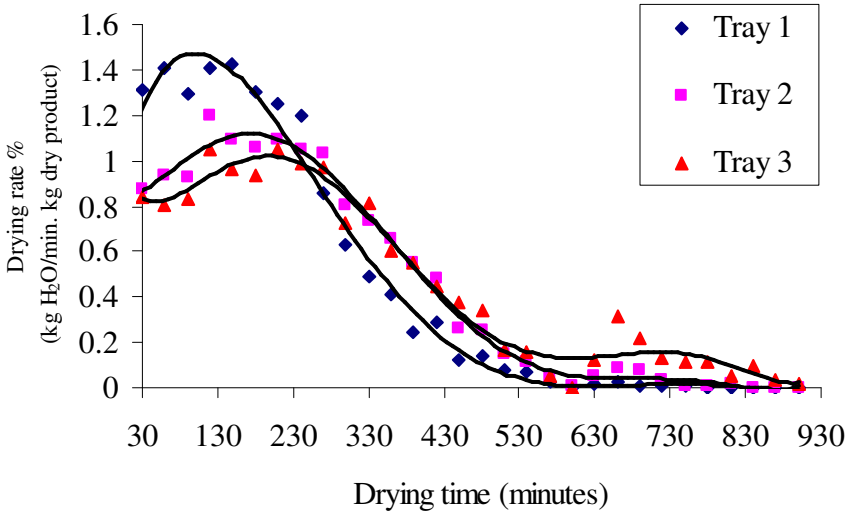

Figure 5.6 Drying rate curves plotted for potato on a dry basis

During the initial stages of drying, the rate of moisture migration is sufficient to maintain the surface in a completely wet condition, Figure 5.7. Therefore, during this period, the rate of drying of the material is controlled by the rate of evaporation from the surface. This is controlled by the condition of air adjacent to the surface. Thus, during this period, the rate of drying is relatively constant as shown in Figure 5.7, which is known as the constant rate period.

The point where the drying rate starts to decrease is known as the critical moisture content. Thereafter, the period of drying is known as the falling rate period. This is the period when the

surface of the material is not wetted completely (by migration of moisture). The drying rate tends to zero when the rate of evaporation from the surface equals the rate of absorption of moisture by the material and is known as the equilibrium moisture content. Since the drying rate decreases to zero, potato is a hygroscopic material.

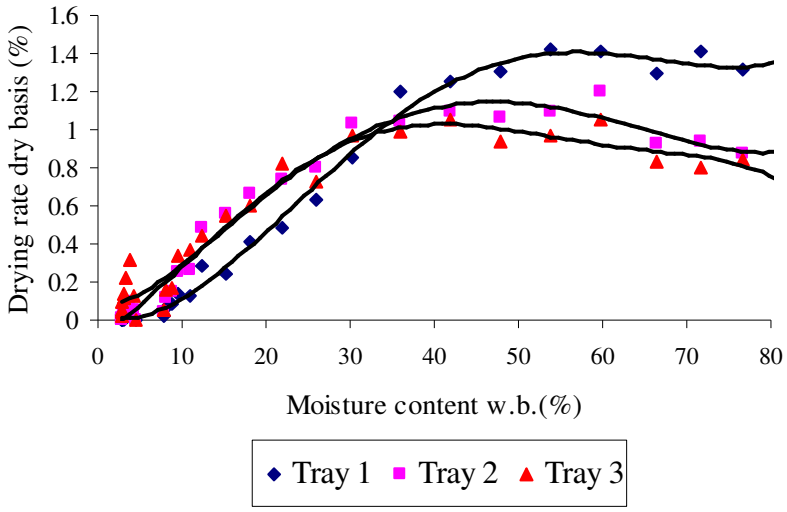

Figure 5.7 Drying rate curves

Figure 5.8 displays the variation of air temperature with vertical distance from the bottom of the drying chamber. Ambient air temperature is included in the graph for comparison.

A major drawback of the shelf-type dryer is the uneven drying: As a result of the migration of the drying front, the materials at the entrance are dried, while at the exhaust are under-dried. This problem can be alleviated by rotating the drying shelves. In such a rotating operation, the hot air from the collector is used to heat the product already in the latter

stages of drying (falling rate period), while the unsaturated air is used to remove moisture from product in the upper shelves.

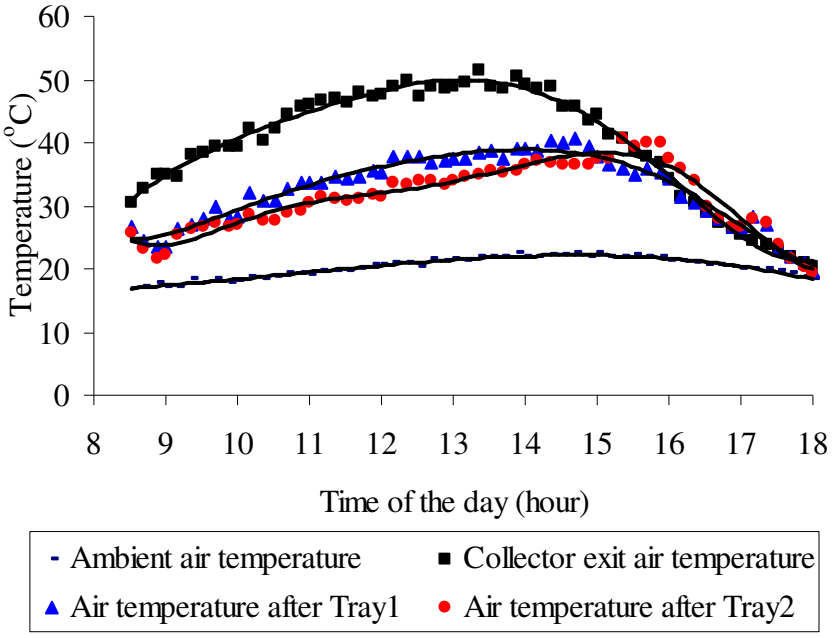

Figure 5.8 Temperature variations with respect to the vertical distance from the drying chamber bottom

5.4 Metrological Data during the Test

The weather through out the experiments was clear and hot at the daytime. On November 2, 2004 the maximum temperature reached 22.65^{0}C at 2:41pm and radiation reached 1.0357 kW/m^2 around the noon. The sunrise was at 7:00 am and sunset was at 5:30 PM. This is shown in Figure 5.9.

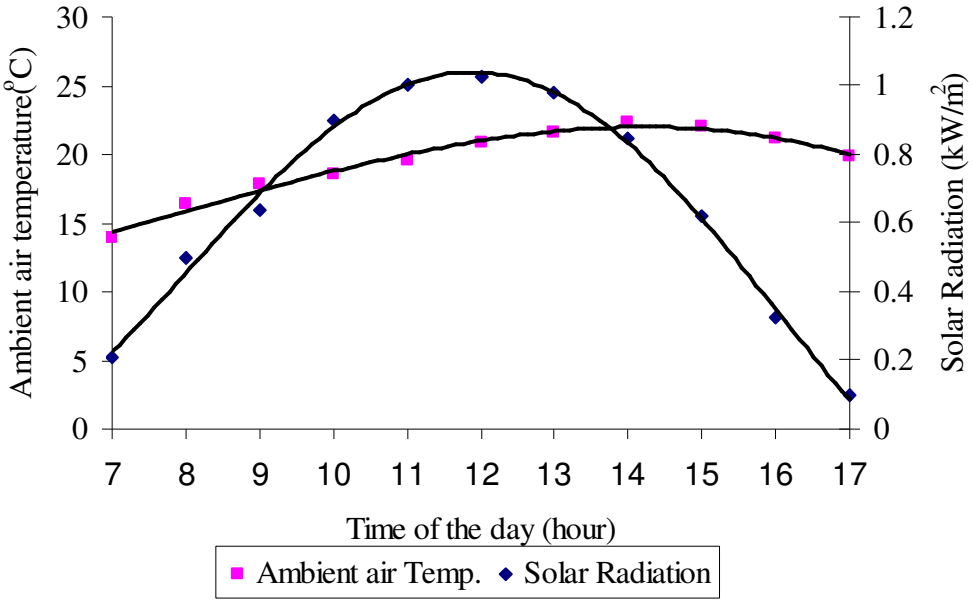

Figure 5.9 Weather data for the test period: measured total solar radiation and ambient temperature obtained from the pyranometer and temperature sensor.

Chapter 6

Conclusions and Recommendations for Future Work

6.1 Conclusions

1. Solar energy was utilized to dry potato slices in the shelf or batch type solar dryer with $2m^2$ flat plate collector. It produced temperatures of 14-29^oC (from 8:30AM- 4:00 PM) higher than the ambient air temperature in a clear day, and dried 6.3kg/m^2 of tray area 7mm x 10mm x 49.7mm slices on a sunny day from 8:30 am to 10 am of the next day. The final moisture content of the potato of 2.62-2.93% which was observed after 13 sunny hours.
2. The collector performance is encouraging. Thermal efficiency lies between 14.59% and 29.95% and temperature rise is between 14 and 29^oC for air flow rates ranging from 0.00595 to 0.0114 kg/s.m^2 of collector area.
3. The drying time required by traditional open sun drying is reduced by 3 hours (about 19%) in natural convection dryer under the existing environmental conditions. Further more the drying material is protected from direct solar radiation, infestation by insects and contamination by dust. As a result, the product quality is high.
4. Since when the moisture content reaches equilibrium moisture, the drying rate is zero. Potato is a hygroscopic material.
5. The system drying efficiency (η_s) or system efficiency is about 16% and dryer efficiency (η_d) is about 65%.

6.2 Recommendations for Future work

- The conducted experiments will form possible bases for the future work and the study can be developed for other agricultural products and different seasons.
- Use of wind energy or photovoltaics to provide fan power can be considered where and when feasible.
- Modeling and simulation to investigate the design and optimization of the solar dryer and the dryer operation can be carried out.
- The effects of the location of trays and number of trays in the chamber and use of other designs of collector can be taken as a future work.
- The possible use of side reflectors to increase the amount of incoming solar energy to the unit must increase the dryer performance and hence can be taken as a future work.
- The improvement of air distribution in the drying chamber can be studied for the performance improvement of the dryer.

References

[1] Ambrose Osakwe and Herbert Weingartmann, *Performance of an Indirect Forced Convection Solar Dryer with Porous Air Heater*, Dept. of Agricultural Engineering, Universität für Bodenkultur ,A-1190 Vienna.

[2] Carl W.Hall, P.E., *Drying and Storage of Agricultural Crops*, AVI Publishing Company Inc., Westport.

[3] Delta-T Device Ltd., "*User Manual-Dome Solarimeter and Albedometer*", 128 Low Road, Burwell, Cambridge CB5 OEJ,U.K (1996).

[4] Delta-T Device Ltd., "*User Manual for DL2e Data Logger Hardware Reference*", version 3,128 Low Road, Burwell, Cambridge CB5 OEJ, U.K (1992).

[5] Delta-T Device Ltd., "*User Manual for DL2e Data Logger, Getting Started*", version 5.0,128 Low Road, Burwell, Cambridge CB5 OEJ,U.K (1996).

[6] Delta-T Device Ltd., "*User Manual-Relative Humidity and Air temperature sensors*", 128 Low Road, Burwell, Cambridge CB5 OEJ,U.K (1996).

[7] Delta-T Device Ltd., "*User Manual Temperature Probes*", 128 Low Road, Burwell, Cambridge CB5 OEJ,U.K (1996).

[8] *Design and Testing of a New Solar Tray Dryer* http://users.auth.gr/~karapant/tdk/Publications/files/Vlachos_et_al_2002.pdf

[9] Duffie and Beckman; *Solar Engineering of Thermal Processes*; 2nd edition, John Wiley & Sons, INC. ; New York, 1991.

[10] *Field Performance of a Solar Tunnel Drier:* http://wire0.ises.org/wire/doclibs/KoreaConf.nsf/id/DA314E2D0606C68BC12565A0004ED110/$File/1-817.pdf.

[11] Kreith Frank, *Principle of Solar Engineering* , Mc Graw Hill Book Company, Washington, 1978.

[12] *Grain Storage Techniques:* http://www.fao.org/docrep/T1838E/T1838E00.htm

[13] Laszlo Imre, *Solar Drying in Handbook of Drying.*

[14] Garg. H.P, *Advances in Solar Energy Technology*, D.Reidel Publishing Company, Volume III, Holland, 1987.

[15] Yuncu. H. and Paykoc. E., *Solar Energy Utilization*, Martinus Nijhoff Publishers Dordrecht, Netherland, 1987

[16] *Indirect, Through-pass, Solar Food Dryer.* http://www.homepower.com/files/fooddeh.pdf

[17] Cicala L. and Farina G.; *Performance Analysis of Solar Air Heaters of Conventional Design*, Journal of Solar Energy, Volume 41,No. 1 PP.101-107,1998.

[18] Biondi P. et al, *Performance Analysis of Solar Air Heaters of Conventional Design*, Journal of Solar Energy, Vol.41, No.1, pp. 101-107, 1988.

[19] Proceeding of Energy Conference 2002, *Energy in Ethiopia*: Status, Challenges and Prospects UNCC, Addis Ababa, 21-22 March 2002

[20] Solar Air Heating: http://www.courses.ait.ac.th/ED06.22/course1/lecs/module3/m32o98.html

[21] Solar Drying in Thailand: http://www.ieiglobal.org/ESDVol2No2/dryingthailand.pdf

[22] Janjai S., *Investigation of the Performance of a Solar Dryer for Lemon-grass*, Kingmongkut's University of Technology Thonburi, International Symposium

[23] Nejat T. Veziroglu, *Alternative Energy Sources VIII*, Hemispheric Publishing Company, Volume I, New York, 1989.

[24] Klein S.A., *Calculation of Flat Plate Collector Loss Coefficients,* Journal of Solar Energy. Vol. 17, pp. 79-80, 1975.

Appendix A

Raw data of the experiment is presented in the following tables.

Table A.1 Raw data of the efficiency analysis

Hour	Air flow velocity (m/s)	Air mass flow rate (kg/s)	$(T_o-T_a)/I_T$ ($^oCm^2/W$)	Ambient Temp. T(^oC)	Collector Exit temp. T(^oC)	Global Solar radiation I_T(kW/m^2)	Useful energy (kW)	Collector efficiency (%)
8:30	0.12	0.011904	0.024404	16.68	30.58	0.569574	0.166293	14.59801
8:40	0.13	0.012896	0.025804	17.22	32.65	0.597972	0.19998	16.72155
8:50	0.13	0.012896	0.026921	17.64	34.83	0.63854	0.222791	17.44533
9:00	0.14	0.013888	0.026657	17.23	35.03	0.667748	0.248442	18.60299
9:10	0.14	0.013888	0.025196	17.17	34.7	0.69574	0.244674	17.58371
9:20	0.15	0.01488	0.026785	18.34	38.04	0.735497	0.294602	20.02739
9:30	0.17	0.016864	0.026154	17.83	38.53	0.791481	0.35083	22.1629
9:40	0.16	0.015872	0.025631	18.35	39.26	0.815822	0.333543	20.44215
9:50	0.18	0.017856	0.025939	17.77	39.51	0.838134	0.39013	23.27375
10:00	0.21	0.020832	0.024581	18.11	39.41	0.866531	0.44594	25.73133
10:10	0.18	0.017856	0.026313	18.82	42.24	0.890061	0.420278	23.60954
10:20	0.22	0.021824	0.023993	18.3	40.2	0.912779	0.480335	26.3117
10:30	0.2	0.01984	0.025274	18.83	42.32	0.929412	0.468372	25.19722
10:40	0.19	0.018848	0.026361	19.44	44.4	0.946856	0.472798	24.96675
10:50	0.19	0.018848	0.027292	19.21	45.76	0.972819	0.502916	25.8484
11:00	0.18	0.017856	0.027346	19.18	46.16	0.986613	0.484164	24.53667
11:10	0.19	0.018848	0.026937	19.71	46.56	0.996755	0.508599	25.51276
11:20	0.2	0.01984	0.027066	19.79	47.12	1.009736	0.544938	26.98419
11:30	0.22	0.021824	0.02588	19.73	46.24	1.024341	0.581447	28.38152
11:40	0.21	0.020832	0.027361	19.86	47.92	1.025558	0.587469	28.64142
11:50	0.23	0.022816	0.025862	20.77	47.44	1.031237	0.611545	29.65104

Continued…

12:00	0.23	0.022816	0.026118	20.71	47.76	1.0357	0.620259	29.94394
12:10	0.22	0.021824	0.027187	20.88	48.96	1.03286	0.615882	29.8144
12:20	0.21	0.020832	0.028331	20.91	50	1.026775	0.609033	29.65757
12:30	0.23	0.022816	0.026254	20.43	47.44	1.028803	0.619341	30.10009
12:40	0.23	0.022816	0.027135	21.47	48.88	1.010142	0.628513	31.11016
12:50	0.22	0.021824	0.026975	21.29	48.56	1.010953	0.598116	29.58179
13:00	0.21	0.020832	0.027317	21.43	48.88	1.004868	0.574698	28.59567
13:10	0.21	0.020832	0.028302	21.31	49.44	0.993915	0.588934	29.627
13:20	0.2	0.01984	0.029895	21.95	51.36	0.983773	0.586412	29.80423
13:30	0.21	0.020832	0.028398	21.76	48.96	0.957809	0.569464	29.7274
13:40	0.2	0.01984	0.028346	22.03	48.72	0.941582	0.532177	28.25974
13:50	0.19	0.018848	0.030039	22.45	50.32	0.927789	0.52792	28.45045
14:00	0.2	0.01984	0.030118	21.91	49.12	0.903448	0.542546	30.02638
14:10	0.18	0.017856	0.031187	22.05	48.72	0.855172	0.478601	27.9827
14:20	0.19	0.018848	0.031623	22.36	48.8	0.836105	0.500833	29.95034
14:30	0.19	0.018848	0.029194	22.15	45.6	0.803245	0.444196	27.65005
14:40	0.18	0.017856	0.031152	22.65	45.84	0.744422	0.416151	27.95129
14:50	0.18	0.017856	0.029605	21.81	43.44	0.730629	0.388156	26.56317
15:00	0.17	0.016864	0.031811	22.49	44.48	0.691278	0.372694	26.95685
15:10	0.16	0.015872	0.029781	21.93	41.2	0.647059	0.307383	23.7523
15:20	0.14	0.013888	0.035263	21.81	40.55	0.53144	0.261562	24.60883
15:30	0.16	0.015872	0.029332	22.08	38.87	0.572414	0.267823	23.39421
15:40	0.15	0.01488	0.028798	22.02	37.78	0.547262	0.235681	21.53278
15:50	0.15	0.01488	0.030969	22.04	36.89	0.479513	0.222073	23.15607
16:00	0.13	0.012896	0.03645	21.32	34.17	0.352535	0.166542	23.62062
16:10	0.13	0.012896	0.02893	21.23	31.37	0.350507	0.131419	18.74702
16:20	0.12	0.011904	0.030615	21.1	30.39	0.303448	0.111141	18.31302
16:30	0.12	0.011904	0.0332	20.73	29.04	0.250304	0.099417	19.8592

Continued…

16:40	0.11	0.010912	0.034695	20.57	27.4	0.196856	0.074902	19.02447
16:50	0.07	0.006944	0.036897	20.29	26.21	0.160446	0.041314	12.87472
17:00	0.06	0.005952	0.031799	20.07	25.33	0.165416	0.031464	9.510595
17:10	0.05	0.00496	0.041982	20.13	24.49	0.103854	0.021734	10.4636
17:20	0.04	0.003968	0.060864	19.95	23.95	0.06572	0.015951	12.13583
17:30	0.03	0.002976	0.067899	19.58	22.82	0.047718	0.00969	10.15386

Table A.2 Percentage Moisture content on wet basis and percentage drying rate on dry basis on Tray1, Tray2 and Tray3.

Drying Time (minutes)	Mass of potato on T1(gm)	Mass of potato on T2(gm)	Mass of potato on T3(gm)	Moisture content on wet basis T1 (%)	Moisture content on wet basis T2 (%)	Moisture content on wet basis of T3 (%)	Drying rate on dry basis of T1 (%)	Drying rate of on dry basis of T2 (%)	Drying rate on dry basis of T3 (%)
0	2450	2610	2810	81.55918	81.55939	81.55872			
30	2272	2484	2679	74.29388	76.7318	76.8968	1.313265	0.872637	0.84266
60	2081	2349	2554	66.49796	71.55939	72.4484	1.409178	0.934968	0.804065
90	1906	2215	2425	59.3551	66.42529	67.85765	1.291132	0.928042	0.829795
120	1715	2042	2262	51.55918	59.79693	62.05694	1.409178	1.198144	1.048501
150	1522	1884	2112	43.68163	53.7433	56.71886	1.423934	1.094259	0.964878
180	1345	1731	1966	36.45714	47.88123	51.52313	1.305888	1.05963	0.939148
210	1175	1573	1803	29.51837	41.82759	45.72242	1.254242	1.094259	1.048501
240	1013	1422	1649	22.90612	36.04215	40.24199	1.195219	1.045779	0.990609
270	897	1273	1498	18.17143	30.33333	34.86833	0.855836	1.031927	0.971311
300	812	1157	1385	14.70204	25.88889	30.84698	0.627121	0.80338	0.726875
330	746	1051	1258	12.00816	21.82759	26.3274	0.486941	0.734123	0.81693
360	690	956	1164	9.722449	18.18774	22.98221	0.413162	0.65794	0.604657

390	657	876	1079	8.37551	15.12261	19.9573	0.243471	0.554055	0.546764
420	618	806	1010	6.783673	12.44061	17.50178	0.287738	0.484798	0.443844
450	601	768	952	6.089796	10.98467	15.43772	0.125424	0.263176	0.373086
480	582	732	899	5.314286	9.605364	13.5516	0.14018	0.249325	0.340924
510	571	710	873	4.865306	8.762452	12.62633	0.081157	0.152365	0.167246
540	562	693	849	4.497959	8.111111	11.77224	0.066401	0.117737	0.154381
570	559	687	841	4.37551	7.881226	11.48754	0.022134	0.041554	0.05146

Continued…

600	525	599	810	2.987755	4.509579	10.38434	0.00209	0.005079	0.001662
630	523	591	791	2.906122	4.203065	9.708185	0.014756	0.055405	0.122218
660	519	578	742	2.742857	3.704981	7.964413	0.029512	0.090034	0.315194
690	518	567	708	2.702041	3.283525	6.754448	0.007378	0.076183	0.218706
720	517	562	687	2.661224	3.091954	6.007117	0.007378	0.034628	0.135083
750	516	561	669	2.620408	3.05364	5.366548	0.007378	0.006926	0.115785
780	516	560	651	2.620408	3.015326	4.725979	0	0.006926	0.115785
810	516	558	643	2.620408	2.938697	4.441281	0	0.013851	0.05146
840	516	558	628	2.620408	2.938697	3.907473	0	0	0.096488
870	516	558	622	2.620408	2.938697	3.69395	0	0	0.038595
900	516	558	619	2.620408	2.938697	3.587189	0	0	0.019298
Final dry mass	451.8	481.3	518.2						

Tables A.3 Relative Humidity of the drying air at the exit of the collector and tray2 and temperature of drying air at the exit of the collector, Tray1 and Tray2.

Hour	Cold Junction Temp. (^oC)	Relative humidity at the exit of the collector (%)	2-Nov-04 08:31:56Relative humidity from the exit of T2 (%)	Ambient air Temp. (^oC)	Air temp. at the exit of the collector (^oC)	Global radiation on the collector plane (KW/m^2)	Air temp. at exit of T1 (^oC)	Air temp. at the exit of T2 (^oC)
8:31	15.44	19.6544	25.0304	16.68	30.58	0.56957	26.64	25.85
8:41	15.75	17.2608	31.3856	17.22	32.65	0.59797	24.48	23.17
8:51	16.41	15.264	33.1776	17.64	34.83	0.63854	23.34	21.44
9:01	16.99	15.0144	34.048	17.23	35.03	0.66775	23.54	22.25
9:11	17.47	15.008	35.9424	17.17	34.7	0.69574	26.31	25.24
9:21	17.91	13.248	43.4176	18.34	38.04	0.7355	27.09	26.28
9:31	18.41	12.7808	42.496	17.83	38.53	0.79148	27.92	26.73
9:41	18.82	12.2368	41.216	18.35	39.26	0.81582	29.74	27.33
9:51	19.21	11.5008	43.8272	17.77	39.51	0.83813	28.01	26.79
10:01	19.51	11.2512	43.008	18.11	39.41	0.86653	28.23	27.1
10:11	19.82	9.7152	39.8336	18.82	42.24	0.89006	32.01	28.43
10:21	20.14	10.8864	37.7344	18.3	40.2	0.91278	30.68	27.7
10:31	20.42	9.9392	39.0144	18.83	42.32	0.92941	30.86	27.76

Continued…

10:41	20.79	9.1904	39.7824	19.44	44.4	0.94686	32.6	28.97
10:51	21.1	8.7488	41.6768	19.21	45.76	0.97282	33.53	29.32
11:01	21.38	8.7168	42.0352	19.18	46.16	0.98661	33.77	30.36
11:11	21.73	8.4416	36.352	19.71	46.56	0.99676	33.8	31.37
11:21	22.12	8.2624	39.5264	19.79	47.12	1.00974	34.58	31.13
11:31	22.47	8.416	35.4304	19.73	46.24	1.02434	34.26	30.78
11:41	22.77	7.872	35.328	19.86	47.92	1.02556	34.75	31.17
11:51	23.28	7.7504	36.2496	20.77	47.44	1.03124	35.71	31.75
12:01	23.79	7.5648	37.0688	20.71	47.76	1.0357	35.21	31.5
12:11	24.26	7.3408	29.696	20.88	48.96	1.03286	37.65	33.79
12:21	24.72	7.0592	30.5664	20.91	50	1.02678	37.93	33.4
12:31	24.96	7.5456	28.5184	20.43	47.44	1.0288	37.9	33.85
12:41	24.97	7.2768	28.3648	21.47	48.88	1.01014	36.91	34.12
12:51	25.2	7.3152	27.904	21.29	48.56	1.01095	37	33.36
13:01	25.41	7.264	26.4192	21.43	48.88	1.00487	37.42	34.04
13:11	25.63	7.1424	25.1968	21.31	49.44	0.99392	37.41	34.72
13:21	25.81	6.6688	28.2624	21.95	51.36	0.98377	38.49	34.85
13:31	26.04	7.2704	26.5216	21.76	48.96	0.95781	38.76	35.69
13:41	26.1	7.5072	25.6512	22.03	48.72	0.94158	37.59	35.22
13:51	26.13	7.008	27.9552	22.45	50.32	0.92779	39.13	35.42
14:01	26.29	7.5904	23.904	21.91	49.12	0.90345	39.02	36.46
14:11	26.38	7.7568	23.1424	22.05	48.72	0.85517	38.81	36.99

14:21	26.44	7.7056	24.5376	22.36	48.8	0.83611	40.37	36.69
14:31	26.51	8.448	22.7072	22.15	45.6	0.80325	39.92	36.41

Continued…

14:41	26.5	8.3328	19.9168	22.65	45.84	0.74442	40.53	36.58
14:51	26.4	9.0688	20.1728	21.81	43.44	0.73063	39.44	36.35
15:01	26.19	8.9472	22.5408	22.49	44.48	0.69128	37.67	37.31
15:11	26.18	10.4128	20.0896	21.93	41.2	0.64706	36.35	37.49
15:21	26.03	11.04	21.1776	21.81	40.55	0.53144	35.72	40.75
15:31	25.86	12.6144	19.3152	22.08	38.87	0.57241	34.79	39.39
15:41	25.73	13.8624	16.7232	22.02	37.78	0.54726	35.73	39.95
15:51	25.65	15.1488	17.344	22.04	36.89	0.47951	35.13	39.9
16:01	25.42	17.5296	17.984	21.32	34.17	0.35254	34.16	37.58
16:11	25	19.9488	19.4944	21.23	31.37	0.35051	31.44	35.72
16:21	24.68	21.4848	20.96	21.1	30.39	0.30345	30.49	33.87
16:31	24.34	23.296	22.784	20.73	29.04	0.2503	29.35	29.91
16:41	23.99	25.9456	26.08	20.57	27.4	0.19686	27.92	27.98
16:51	23.65	27.4944	29.1328	20.29	26.21	0.16045	26.75	26.81
17:01	23.27	28.8768	30.8224	20.07	25.33	0.16542	26.82	26.56
17:11	22.92	31.232	30.5664	20.13	24.49	0.10385	28.22	27.91
17:21	22.62	33.2288	30.976	19.95	23.95	0.06572	27.02	27.28
17:31	22.31	35.2256	34.304	19.58	22.82	0.04772	23.31	23.7
17:41	21.96	37.4272	38.0416	19.21	21.86	0.03357	21.92	21.74
17:51	21.58	39.168	42.1376	18.85	20.97	0.01623	21.01	20.39
18:01	21.21	40.3456	45.5168	18.38	20.23	0.00472	19.78	19.25

8:01	14.91	30.976	28.3136	15.75	24.96	0.37404	25.24	27.32
8:11	15.29	28.5696	27.136	15.72	26.15	0.42637	26.46	28.88
8:21	15.69	25.6704	26.2656	16.48	28.43	0.47708	27.72	36.14

Continued…

8:31	16.13	22.4896	20.1984	16.51	30.38	0.53306	28.4	38.91
8:41	16.55	21.0112	17.12	16.63	31.62	0.5712	29	38.96
8:51	16.99	18.0032	14.6752	17.38	32.61	0.64219	30.09	36.65
9:01	17.5	15.7568	13.6768	17.85	34.61	0.68722	30.84	34.05
9:11	18.01	14.6496	14.816	18.24	36.41	0.7213	33.11	34.32
9:21	18.47	14.0736	16.1344	17.99	36.67	0.75619	33.91	33.89
9:31	18.9	13.632	16.5824	18.02	37.11	0.82962	33.66	33.84
9:41	19.28	11.7248	16.9984	18.79	39.66	0.83164	36.04	34.43
9:51	19.7	11.5072	17.0624	18.66	40.88	0.83489	39.17	35.4
10:01	20.03	11.9616	17.0688	18.44	38.81	0.87221	38.07	34.88
10:11	20.33	12.102	17.734	18.9	31.14	0.897	37.89	34.68
10:21	20.64	11.322	17.965	19.09	20.97	0.9262	36.02	34.7
10:31	20.9	10.746	17.613	19.06	21.14	0.9554	35.45	35.06
10:41	21.19	9.216	17.261	19.65	21.62	0.9663	36.45	36.08
10:51	21.55	8.9536	17.005	19.62	21.89	0.9728	37.15	37.16
11:01	21.87	9.0432	16.666	19.74	22.21	1.0012	37.17	37.2
11:11	22.16	8.5184	16.243	19.64	22.51	1.0178	37.21	37.28
11:21	22.48	8.0128	15.789	19.85	22.86	1.0292	38.09	38.08
11:31	22.91	8.128	15.053	20.28	23.4	1.0231	37.93	37.99
11:41	23.34	8.064	15.053	20.41	23.98	1.0511	38.11	38.08
11:51	23.78	8.4352	14.835	20.71	24.33	1.0377	37.97	38.09
12:01	24.2	8.0576	14.592	20.57	24.57	1.0531	38.06	38.07

12:11	24.52	8.4992	14.893	20.57	24.77	0.9761	37.9	38.11
12:21	24.77	7.9424	14.726	20.94	25.18	1.0596	38.26	38.39
12:31	25.12	7.4304	14.112	21.49	25.29	1.0807	40.04	39.93

Continued…

12:41	25.44	7.3472	13.286	21.59	25.7	1.0787	40.43	40.64
12:51	25.78	7.6864	13.171	21.45	26.03	1.0434	39.95	40.53
13:01	25.92	8.3072	13.165	21.34	25.86	1.056	39.37	40.24

Appendix B

Dimension of the sliced potato and the trays used in the drying chamber

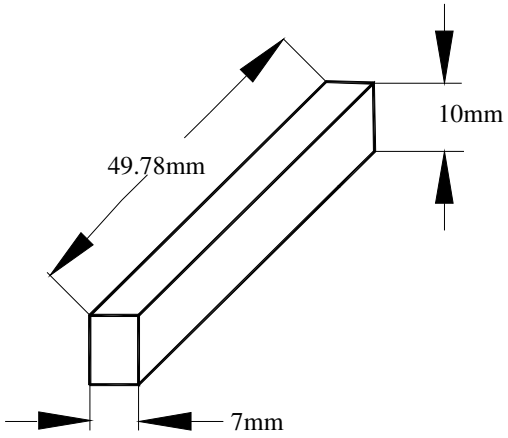

Figure B.1 Sample of sliced potato

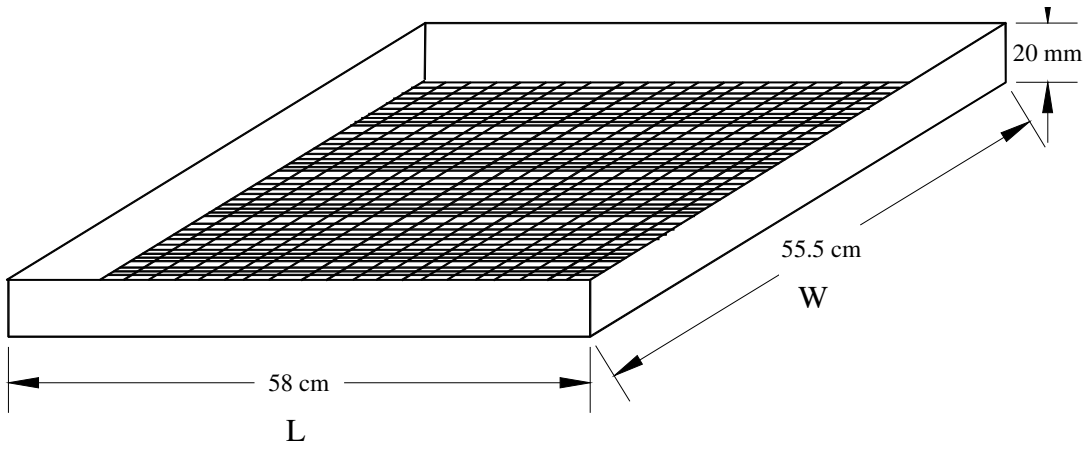

Figure B.2 Dimension of trays used in the drying chamber (T1= 92.5 cm x 42 cm, T2 = 96 cm x 44 cm, T3 = 102 cm x 44 cm)